PHYSICAL REVIEW B, VOLUME 64, 125209

Energy levels of isolated interstitial hydrogen in silicon

Conyers Herring,* N. M. Johnson, and Chris G. Van de Walle
Xerox Palo Alto Research Center, Palo Alto, California 94304

(Received 17 August 2000; published 11 September 2001)

This paper first describes the quantitative determination of the static and dynamic properties of the locally stable states of monatomic hydrogen dissolved in crystalline silicon: H^+, H^0, and H^-. The monatomic hydrogens were created controllably near room temperature by using hole-stimulated dissociation of phosphorus-hydrogen (PH) complexes. Drift velocities and charge-change rates were studied via time-resolved capacitance-transient measurements in Schottky diodes under changes of bias. These data enable the donor level ε_D of ^2H to be located at ~0.16 eV below the conduction band (confirming that the $E3'$ center found in proton-implanted Si corresponds to interstitial H in undamaged Si), and the acceptor level ε_A at ~0.07 eV below midgap, so that hydrogen is a "negative-U" system. The experimental values of ε_D and ε_A are consistent with predictions from first-principles calculations, which also provide detailed potential-energy surfaces for hydrogen in each charge state. While the phonon-mediated reaction $H^0 \rightarrow H^+ + e^-$ is fast, the reaction $H^- \rightarrow H^0 + e^-$ has an activation energy ~0.84 eV, well above the energy difference (~0.47 eV) between initial and final states. Our experiments also yielded diffusion coefficients near room temperature for $^1H^+$, $^2H^+$, and $^2H^-$. The asymmetrical positioning of ε_D and ε_A in the gap accounts for many previously unexplained effects. For example, it is shown to be responsible for the much greater difficulty of passivating phosphorus-doped than comparably boron-doped Si. And while modest hole concentrations dissociate PH complexes rapidly at temperatures where thermal dissociation takes years, we could not detect an analogous dissociation of BH complexes by minority electrons, a process that is expected to be frustrated by the rapid thermal ionization of H^0. The distribution of hydrogen in n-on-n epitaxial layers hydrogenated at 300 °C can be accounted for if the donor-hydrogen complexes are in thermal equilibrium with H_2 complexes whose binding energy (relative to $H^+ + H^-$) is of the order of 1.75 eV. With this binding energy, the measured migration of H_2 at 200 °C and below must be by diffusion without dissociation.

DOI: 10.1103/PhysRevB.64.125209 PACS number(s): 71.55.Cn, 61.72.Tt

I. INTRODUCTION

A number of attributes of hydrogen dissolved in crystalline silicon, especially its high reactivity for formation of complexes with other impurities or with lattice defects and its high mobility even at room temperature, have stimulated considerable research both by workers interested in devices and device reliability and by those concerned with the fundamentals of defect kinetics in solids.[1] Unfortunately, these same attributes, combined with the low equilibrium solubility of hydrogen in silicon, have conspired throughout much past history to thwart the efforts of experimentalists to disentangle the various mechanisms and material parameters involved. Thus, although it has been known for some time that hydrogen dissociates into monatomic species in intrinsic silicon at high temperatures,[2] and that it forms complexes with acceptors,[3] with donors,[4] and probably with itself,[5] it has only fairly recently been established that H^+ has high mobility,[6] and that there is a stable H^- species[7] also of high mobility.[8] Indeed, doubts continue to be expressed about the H^- species.[9] Other properties of the monatomic species, such as donor and acceptor energies and temperature-dependent rates of charge change by emission and absorption of electronic carriers, were not established up to the time of the present work.

Since migration of hydrogen in silicon is normally dominated by drift and diffusion of the monatomic species, and since both drift and the kinetics of complex formation depend on charge state, it is clear that an adequate understanding of phenomena involving hydrogen will be possible only when the energetic and kinetic descriptors of these species are reliably known. To this end we developed an experimental technique to study the kinetics of H^+ and H^-, which involves their release at a sharply defined time by hole-induced dissociation of donor-hydrogen complexes. Results for the mobility of H^- and bounds on some charge-change rates, obtained by this method, have been previously published.[8] Here we provide detailed descriptions of the experimental techniques and analyses for determining ε_A, which establishes the negative-U character of isolated hydrogen in silicon. This includes an extension of previous work on the diffusion coefficient of H^+ as well as that of H^-, near room temperature, on the isotope effect for H^-, and on some of the charge-change rates. We also undertake to resolve several controversies and uncertainties about these species, and to show that a straightforward model based on three hydrogen species, H^+, H^0, and H^-, fits nicely a variety of experimental data on hydrogen redistribution in n-type Schottky diodes subjected to various sequences of hole injection, electron flooding, and reverse bias. The model uses universal migration and charge-change parameters, and assumes recombination of hydrogen with donors to occur only via the H^- species. It also assumes that near and above room temperature charge change $H^+ \leftrightarrow H^-$ occurs through the ground-state configuration of H^0, although H^0 never achieves a large relative abundance in equilibrium.

 ©2001 The American Physical Society

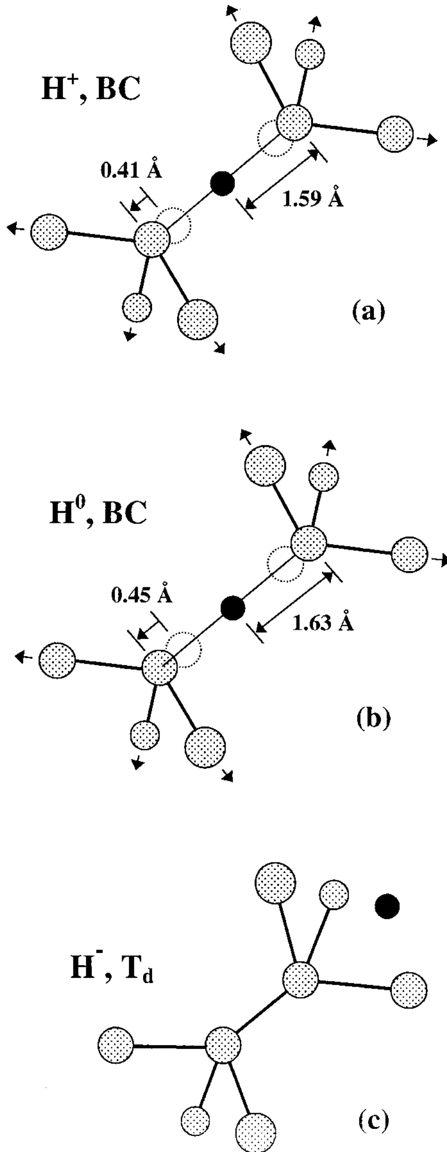

FIG. 1. Schematic illustration of the minimum-energy atomic configurations for hydrogen interstitials in silicon, as derived from first-principles calculations (Ref. 10): (a) the positive charge state, (b) neutral, and (c) the negative charge state.

II. BACKGROUND

A. Theory

1. Interstitial hydrogen

First-principles calculations have produced a wealth of information about the energetics and atomic configurations of isolated hydrogen in silicon.[10] Hydrogen in the positive charge state (H^+) behaves essentially as a proton, seeking out the regions of highest electronic charge density. In a silicon crystal, the maximum charge occurs at the bond center (BC), midway between two Si atoms. The Si atoms have to move outward in order to accommodate the hydrogen; the relaxations are illustrated in Fig. 1(a). The energy gained by forming the three-center Si—H—Si bond suffices to compensate for the strain energy required to move the Si atoms.

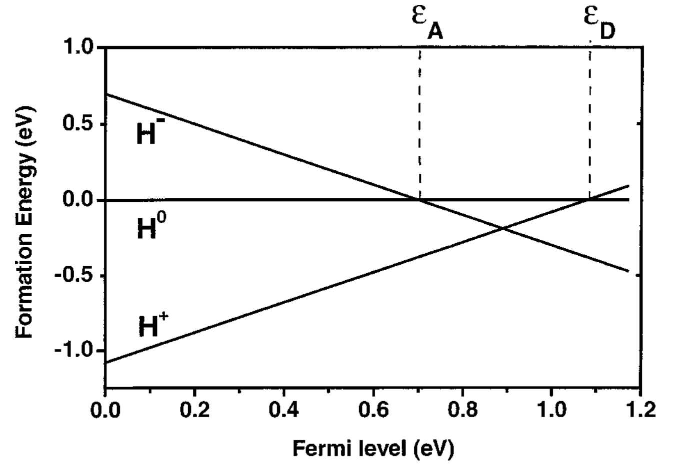

FIG. 2. First-principles results for relative formation energies for different charge states of hydrogen interstitials in Si, as a function of Fermi level ε_F, with $\varepsilon_F = 0$ corresponding to the top of the valence band. The formation energy of H^0 is chosen as the reference. The band-gap error was addressed with a simple correction scheme, as discussed in Ref. 10.

The process of moving the host atoms introduces a level in the band gap, derived from an antibonding combination of Si hybrid orbitals.[11] This level is empty in the positive charge state, but is occupied with one electron when the hydrogen interstitial assumes the neutral charge state (H^0). The wave function corresponding to this level has zero amplitude at the proton, and is antibonding with respect to the Si atoms. This theoretical prediction was confirmed in a number of experiments in which the defect state was probed with electron-spin resonance[12] or with muon-spin rotation.[13] The latter experiment was performed on muonium, a pseudoisotope of hydrogen. Theory and experiment thus agree that the stable state of neutral interstitial hydrogen is also at the bond center, with host-atom relaxations as illustrated in Fig. 1(b).

Interstitial hydrogen in the negative charge state (H^-) assumes an entirely different configuration from that of H^+. Coulomb repulsion now drives the impurity toward the regions of *lowest* charge density in the crystal, which occur at the tetrahedral interstitial site. Relaxations of the host atoms are negligible for this configuration, which is illustrated in Fig. 1(c).

The relative stability of the various charge states can be addressed by using the total energies obtained from the first-principles calculations.[10] Figure 2 depicts the formation energies for the lowest-energy configuration of each of the charge states, that is, BC for H^+ and H^0, and T_d for H^-. The formation energies of H^+ and H^- depend on the Fermi level, which is the reservoir with which the impurity exchanges electrons. The Fermi-level position for which H^+ and H^0 have equal energies defines the $+/0$ transition level, that is, the donor level ε_D; similarly, the acceptor level ε_A (i.e., the $0/-$ transition) is defined as the point where H^0 and H^- have equal energy. Figure 2 shows the first-principles predictions for these values: ε_A is located approximately at $\varepsilon_C - 0.6\,\text{eV}$, and ε_D is approximately at $\varepsilon_C - 0.2\,\text{eV}$. As discussed in Ref. 10, the error bars on these values are quite large because of the band-gap error associated with the

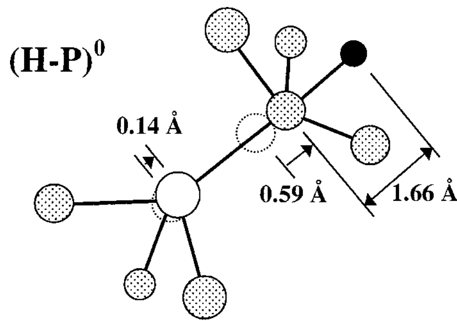

FIG. 3. Schematic illustration of the atomic structure of the hydrogen-phosphorous complex in silicon, as derived from first-principles calculations (Ref. 15).

density-functional calculations. It is thus fortuitous that the calculated donor and acceptor levels are so close to the experimental values, as derived in the present paper. Still, the calculated values were considered sufficiently reliable to predict the negative-U character of the hydrogen interstitial, with $U = \varepsilon_A - \varepsilon_D = -0.4\,\mathrm{eV}$. Broad consensus now exists about the atomic configurations assumed by interstitial hydrogen in silicon, as derived with various computational methods; results from various approaches are reviewed in Ref. 14.

2. Hydrogen-dopant complexes

Computational studies have also produced microstructural models for hydrogen-dopant complexes in silicon. Of particular importance for the present paper are hydrogen-donor complexes, which have been established theoretically as well as experimentally. The structural model for the PH complex as obtained in Ref. 15 is shown in Fig. 3; other computational approaches have produced very similar configurations.[14] The hydrogen is located in an antibonding site of a Si atom adjacent to the P atom. Both the Si and P atoms undergo sizable relaxations along the bond axis.

B. Minority-carrier enhanced dissociation of PH complexes in Si

In the experiments to be reported in this paper, PH complexes provided the source of isolated hydrogen. The hydrogen was released from the complexes by the phenomenon of "minority-carrier-enhanced dissociation," in which the introduction of minority carriers (i.e., holes) destabilizes the PH complexes such that dissociation can occur at temperatures where thermal dissociation in the absence of minority carriers is negligible.[16,17] The dissociation may be expressed by the following initial reaction:

$$\mathrm{PH} + h^+ \rightarrow \mathrm{P}^+ + \mathrm{H}^0. \tag{1}$$

A physical model has been proposed for this reaction.[17] It is envisaged that thermal fluctuations produce a configuration $\mathrm{P}^+ + \mathrm{H}^-$ where the atoms are displaced from their minimum-energy configuration but still in close proximity, hence, a configuration that is of lower energy than for widely separated P^+ and H^-. In such a partially dissociated configuration, the H^- absorbs a hole to become H^0, and the H^0 can then diffuse away without a Coulomb barrier to overcome. The final charge state of the isolated hydrogen is determined by subsequent carrier-capture and -emission processes, the quantitative articulation of which is presented in later sections.

C. Hydrogen donor level

Several studies contributed to the identification and characterization of the donor level for isolated hydrogen in silicon. The level was first reported in 1978, with deep-level transient spectroscopy (DLTS), as one of several deep levels introduced into specimens of n-type silicon by proton bombardment at low temperatures (e.g., 45 K).[18] In the cataloguing of defects generated by the implantation, the particular level of interest was labeled $E3$ and observed to anneal out at 120 K, although in this earliest report neither was the thermal ionization energy quoted nor was the level associated with isolated hydrogen.

A subsequent DLTS study,[19] also on n-type silicon implanted with protons (at 80 K), reported several new observations for this level, now labeled the $E3'$ center. The areal density of the level was found to coincide with the proton-implantation dose, which suggested that the level is associated with a hydrogen-related defect. The electron thermal emission rate was found to depend on the (average) magnitude of the applied electric field in the depletion layer of a Schottky diode. This phenomenon is termed the Poole-Frenkel effect and arises from the electric-field-induced lowering of a Coulomb energy barrier for thermal emission.[20] Observation of the Poole-Frenkel effect thus established that the $E3'$ center is donorlike. By applying a correction for the effect, the zero-field activation energy was estimated to be 0.2 eV. Finally, the authors included in their speculations on the possible origins of this center the suggestion that the level might arise from a hydrogen atom at a single interstitial site.

A third DLTS study[21] further established that $E3'$ is a hydrogen-related defect, reported an activation energy of 0.16 eV after correction for the Poole-Frenkel effect, and quantitatively characterized the annealing stages. In particular, it was observed that the annealing temperature depends on the presence or absence of free electrons.

The application of electron paramagnetic resonance (EPR) techniques contributed decisively to the microscopic identification of the $E3'$ center. Studies of silicon implanted with hydrogen at low temperatures revealed a characteristic paramagnetic defect that was designated the AA9 center.[22] Subsequent studies by Bech Nielsen and co-workers[21,23] clearly established that the paramagnetic center AA9 and the deep level defect center $E3'$ are identical. This conclusion is based on the following observations:

(i) The change between plus and zero charge states occurs for both centers at the same donor energy, $\varepsilon_D \approx \varepsilon_C - 0.16\,\mathrm{eV}$,

(ii) Both centers disappear upon annealing at near 100 K, while illuminating the AA9 center with a standard light intensity, or for the $E3'$ center while in the "electron-

flooding'' regime of an n-type diode (This was interpreted as transitions from either H^+ or H^0 to metastable H^-.)

(iii) Both centers disappear on annealing in the dark at around 200 K (for a given prehistory). (This was interpreted as the migration of H^+ to traps.)

The above observations and interpretations in support of the identity of the AA9 and $E3'$ centers have been further strengthened by the work of Gorelkinskii and Nevinnyi[24] on the effects of uniaxial stress on the AA9 center. These results can be summarized as follows:

(iv) The relative densities of AA9 centers of the four possible orientations can be changed by equilibrating the associated H^+ species in an anisotopic stress field at temperatures from 77 to 170 K, and recovered by similar anneals at zero stress. (This indicates that H^+ as well as H^0 occupies BC sites.)

(v) The coupling constant for the orientation to stress, measured by this effect, is of a sign appropriate to an outward relaxation of the two Si nearest neighbors of an H^+ at a BC site.

(vi) No similar relaxation or recovery occurs when the AA9 centers are reconverted to H^0 by keeping the specimen under illumination. [This was demonstrated at temperatures over the range from 77 to 130 K with measurements on fractional orientation of those AA9 centers that do not disappear due to the process (ii) listed above. This was interpreted as a disappearance of most of the H^0 by conversion to H^+ before there was time for an appreciable probability of a reorientation hop of H^0.]

(vii) From the rates of growth of anisotropy by annealing under stress in the dark (or of loss of anisotropy by annealing under zero stress) one can deduce the hop rate of H^+ between neighboring BC sites.

Some implications of the above studies are discussed later in this paper. Determination of the activation energy for thermal ionization of electrons from the donor level is further discussed in Sec. V B after introduction of the experimental techniques and results from the present study.

D. Negatively charged hydrogen

The existence of negatively charged hydrogen H^- in silicon was originally inferred from the field drift of hydrogen released by the thermal dissociation of PH complexes.[7,25] It was subsequently shown[8] that H^- is the stable form when the Fermi level is positioned 0.3 eV above the midgap energy ε_m, and possibly also at lower positions, which established that the hydrogen acceptor level ε_A is below $\varepsilon_m + 0.3\,\text{eV}$. Since the donor level lies within 0.2 eV of the conduction band (Sec. II C), that is, $\varepsilon_D \geqslant \varepsilon_m + 0.35\,\text{eV}$, the donor level is higher than the acceptor level. This experimentally identifies hydrogen as a ''negative-U'' impurity in silicon, for which two H^0 atoms can lower their energy by changing to H^+ and H^-,[26] as had been tentatively predicted by *ab initio* theoretical calculations (Sec. II A).

With the qualitative information that hydrogen is a negative-U impurity, the fact that H^- is stable for $\varepsilon_F = \varepsilon_m + 0.3\,\text{eV}$ (Ref. 27) imposes a tighter bound on the location of the acceptor level than would apply for the positive-U case. Namely, it is the mean energy $\langle \varepsilon \rangle \equiv (\varepsilon_D + \varepsilon_A)/2$ that is located below $\varepsilon_m + 0.3\,\text{eV}$. This implies that $\varepsilon_A \leqslant \varepsilon_m + 0.25\,\text{eV}$. A direct quantitative determination of ε_A is presented in the present paper.

III. MEASUREMENT STRATEGY

For a negative-U system there is a difficulty with the normal method of locating an acceptor level by measuring the dependence of its charge state on Fermi level ε_F, since the impurity goes from being nearly all positive to nearly all negative when ε_F passes through $\langle \varepsilon \rangle$; the energy separation $\varepsilon_D - \varepsilon_A$ affects the charge-state statistics only in the always-small concentration of H^0. Even for the positive-U case, measurements with ε_F as close to the midgap energy ε_m as expected for ε_A would be difficult since the material would be nearly intrinsic. While in principle the acceptor level can be determined from determinations of ε_D and $\langle \varepsilon \rangle$, however, even the anticipated depth of $\langle \varepsilon \rangle$ presents practical difficulties. The method we developed avoids these difficulties by focusing attention on the kinetics of the transitions

$$H^0 + e^- \rightarrow H^-, \tag{2a}$$

$$H^- \rightarrow H^0 + e^-, \tag{2b}$$

whose rates, related by the principle of detailed balance, are,[1] respectively,

$$r_{0-} = \sigma_{0e} v_e n_e \tag{3}$$

and

$$r_{-0} = r_{0-}[(\nu_0 Z_0)/(\nu_- Z_-)]\exp[(\varepsilon_A - \varepsilon_F)/kT], \tag{4}$$

where σ_{0e} is the cross section for capture of an electron by H^0,v_e is an average thermal velocity for electrons, n_e is the free-electron concentration, ν_0 and ν_- are the number of ground-state configurations for H^0 and H^-, respectively, in a primitive cell, and Z_0 and Z_- are the vibrational partition functions associated with H^0 and H^-, respectively. We obtain ε_A by inserting measured values of r_{-0} and r_{0-} into Eq. (4).

Actually, r_{-0} and r_{0-} cannot be measured directly. In one experiment we measure the spontaneous conversion of H^- to H^+, and in another the absorption of two electrons by H^+. These give the rates of the reactions

$$H^+ + 2e^- \rightarrow H^- \tag{5a}$$

$$H^- \rightarrow H^+ + 2e^-, \tag{5b}$$

instead of the rates of Eq. (2). However, we assume that each of the processes Eq. (5) consists of a fast step and a slow step occurring sequentially, the fast step involving the interconversion of H^0 with H^+, and the slow (hence rate determining) step being the appropriate process of Eq. (2). Specifically, we assume the rates of Eqs. (2a) and (2b) to be essentially the same as those of Eqs. (5a) and (5b), respectively. This assumption is correct provided that (i) the processes (5) both proceed via an essentially equilibrium state of H^0 and (ii) the rates of $H^0 \leftrightarrow H^+ + e^-$ are very fast compared

with the corresponding $H^- \leftrightarrow H^0 + e^-$ rates in Eq. (5). Both of these conditions should be valid if, as *ab initio* calculations suggest,[27] the stable configurations of H^+ and H^0 both have the hydrogen at a bond-center site, with no significant metastable site for H^0, as discussed in detail in later sections.

IV. EXPERIMENTAL TECHNIQUE

A. Test devices

The experiments were performed on Schottky-barrier diodes fabricated on commercial, polished wafers of Czochralski-grown single-crystal silicon. The *n*-type silicon was doped in the melt with phosphorus for a donor concentration of $\sim 1 \times 10^{16}\,\mathrm{cm}^{-3}$. To ensure an Ohmic back contact, the wafers first received a backside implant of phosphorus at 50 kV to a dose of $5 \times 10^{14}\,\mathrm{cm}^{-2}$. The implanted dopant was then activated with a furnace anneal at 900 °C for 30 min. in flowing N_2. The backside contact was completed by vacuum depositing an aluminum film to a thickness of 450 nm, and then annealing the wafer at 450 °C for 30 min in flowing N_2. The wafers were then ready to process Schottky-barrier contacts on the polished front surface. First, a fraction of the phosphorus atoms in the near-surface region of the silicon was passivated by exposure to monatomic hydrogen or deuterium from a remote plasma at 120 °C for 20 min. The hydrogenation system and procedure are described elsewhere.[28] The Schottky diodes were completed with the vacuum evaporation of Pd electrodes through a shadow mask. Control diodes did not receive hydrogenation.

Except for the experimental determination of the diffusion coefficient of $^1H^+$ in Sec. V E, all measurements reported in this paper were made with ^2H. In the text, "hydrogen" or "H" can refer to either species.

B. Measurement technique

The essence of the experiment is the detection of change in space charge in a silicon depletion layer as a consequence of changes in the charge state of hydrogen and the migration of charged hydrogen. A convenient and sensitive way to monitor space charge is with the high-frequency differential capacitance of the depletion layer in a current rectifying device. In Appendix A we derive a useful expression for relating a change in capacitance to the change in the space-charge density. It is based on the depletion approximation which neglects any contribution from free carriers to the space-charge density and specifies that all of the space charge is contained within a layer of thickness W_D. The capacitance of the space-charge layer C is that of a parallel-plate capacitor with the permittivity ϵ_s of the semiconductor and the thickness W_D of the depletion layer

$$C = \epsilon_s / W_D. \tag{6}$$

In Appendix A we show that, for small changes in the charge density, the change in capacitance ΔC is proportional to the first spatial moment of the change $\Delta \rho_s$ in the space-charge density ρ_s within the depletion layer, as follows:

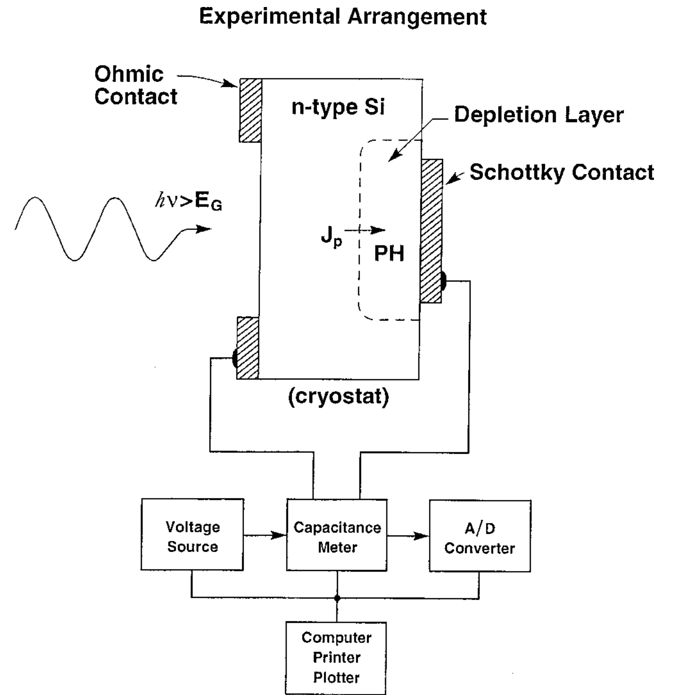

FIG. 4. Schematic diagram of the experimental arrangement for inducing and recording capacitance transients on Schottky barrier diodes.

$$\frac{\Delta C}{C} \cong \frac{\int_0^{W_D} x \Delta \rho_s(x)\, dx}{W_D^2 \rho_s(W_D)}. \tag{7}$$

The measurement system is schematically illustrated in Fig. 4 with a Schottky-barrier diode on *n*-type silicon. An applied reverse bias induces a depletion layer that contains the PH complexes. Minority carriers (holes) are injected into the depletion layer by pulsed illumination of the backside of the diode with strongly absorbed light. A solid-state laser was used for this purpose. The photon energy was 1.53 eV, which yields an absorption depth in Si at room temperature of approximately 13 μm. The diode-depletion capacitance is monitored in real time after hole injection as the space charge relaxes to a new steady state.

The measurement system as described above and schematically depicted in Fig. 4 is essentially a deep-level transient spectrometer[29,30] (DLTS). However, the conventional DLTS algorithm for recording and analyzing data is not applicable in our case. While our measurement involves performing capacitance transient spectroscopy on a deep-level impurity as in conventional DLTS, with isolated hydrogen we have the added complexity that the charge-emitting centers are simultaneously migrating and undergoing chemical reactions as well as capturing and emitting charge. Such a degree of complexity has not been previously encountered in DLTS measurements.

C. Control diodes

The performance of the measurement system was demonstrated with a control diode that was identical to the test

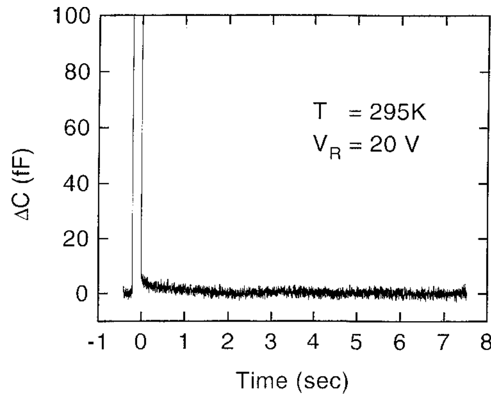

FIG. 5. Capacitance transient recorded on a control Schottky barrier diode that did not receive hydrogenation.

diodes except for the absence of PH complexes in the space-charge layer. In the absence of these complexes the Schottky diode possesses no source of deep levels so that there should be no capacitance change in response to the backside illumination on the recorded time scale of the measurement. Any significant capacitance transient with such a diode would reveal either a temperature-induced capacitance transient or a possible slow recovery of an electronic amplifier from an overload condition. Either response could obscure the interpretation and analysis of data in terms of hydrogen migration and charge changes.

The absence of such artifacts with the diodes and instruments used in the present study is illustrated in Fig. 5. The control diode was mounted in the cryostat and maintained at 295 K with a reverse bias of 20 V. The diode was then backside illuminated under conditions that were empirically identified on test diodes to controllably release a small fraction of the hydrogen from the PH complexes in the depletion layer. Similarly, the time scale for recording the transient response reflects that used on test diodes as reported in later sections. Specifically, the backside was illuminated at an incident power of 230 mW for a duration of 200 msec. Over the recorded time scale the capacitance is essentially unchanged from its preillumination value. The very slight transient at short times arises from heating during the illumination, which can be reliably corrected for by data normalization, as described in later sections.

V. EXPERIMENTAL RESULTS

In this section experimental results are presented for test diodes and the capacitance transients are interpreted in terms of kinetic processes involving the release of hydrogen from PH complexes and the subsequent migration and charge change of the hydrogen.

A. Hole injection

A capacitance transient is illustrated in Fig. 6 for a deuterated diode that was exposed to a single hole injection pulse at 310 K. The diode had a fixed reverse bias of 20 V, and the hole-injection pulse had a duration of 200 msec during which the hole-current density was approximately 0.4 A/cm^2. The graph records the change in capacitance ΔC, with respect to the preinjection quiescent value, with time immediately after the hole-injection pulse. The capacitance relaxes nearly exponentially with a time constant τ_+ from an initial maximum value ΔC_0^+ to a new steady-state ΔC_{SS}^+.

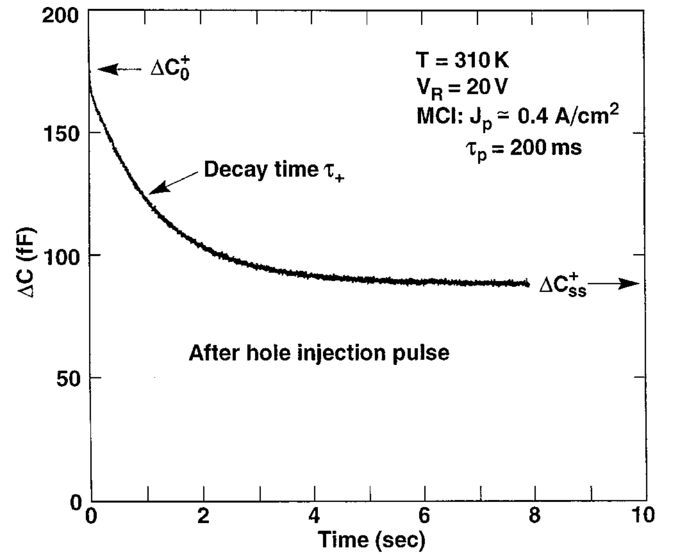

FIG. 6. Capacitance transient $\Delta C(t)$ during a deuterium sweep-out with a 20-V bias.

The interpretation of the ΔC^+ transient depends on the answers to two questions: Was the monatomic hydrogen at the start (i.e., at the conclusion of the hole pulse) mainly H^+, or was it largely or mostly H^0? Were the charge-change times long or short compared with the sweep-out time of H^+? Among the several conceivable combinations of circumstances, the one for which the calculation of the expected ΔC^+ is easiest is the one where all the hydrogen is initially H^+ and gets swept out of the depletion layer by the applied electric field before it has time to change appreciably into H^0 or H^-. This model, which we term the "pure H^+ sweep-out" model, not only is the simplest possibility, but also corresponds closely to the true situation.

A simple and striking success of the pure H^+ sweep-out model is that it predicts the ratio $\Delta C_{SS}^+/\Delta C_0^+$ in Fig. 6 to be close to $\frac{1}{2}$. Since each dissociation event creates at a particular location a new P^+ and a monatomic H which is quickly converted to H^+, that is, is converted on a time scale short compared to the recorded time scale in Fig. 6, the localized charge density created by the hole pulse consists of a $\Delta n_{P^+}(x)$ and an almost identically distributed $n_+(x)$, the density of H^+. If these two distributions were exactly equal and if all of the hydrogen was swept out without recombining, $\Delta C_{SS}^+/\Delta C_0^+$ would be exactly $\frac{1}{2}$. The slight drift of H^+ during the hole pulse will tend to decrease this ratio, and any recombination to increase it. The empirical value in Fig. 6 is 0.50.

B. DLTS of donor level

The phenomenon described above, of H^+ generation and sweep-out in a depletion layer, provides a means to produce

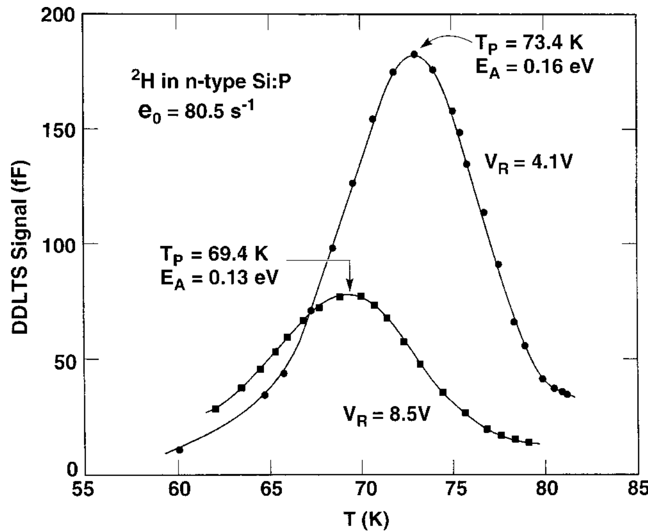

FIG. 7. DLTS spectra for a deuterated n-type Si Schottky diode after minority-carrier (hole) injection at 240 K and immediate quenching to 100 K to freeze-in interstitial, isolated deuterium atoms. The double-correlation technique was used to define the same spatial observation window for two spectra, which were recorded at different reverse biases V_R. Listed are the peak temperature T_p and the emission activation energy E_A for each spectrum and the emission rate window e_0. The width of the trap filling pulse was 2 ms.

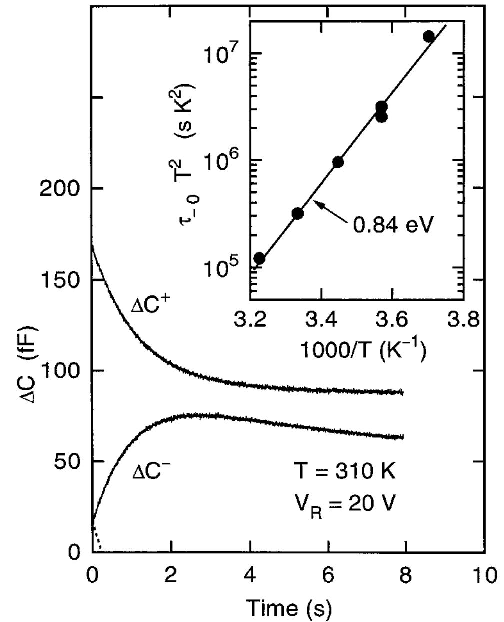

FIG. 8. Capacitance transients $\Delta C(t)$ during deuterium sweep-out with a 20-V bias, with (lower curve) and without (upper curve) a 10-ms flooding at zero bias immediately after the hole pulse. The inset shows an Arrhenius plot of the spontaneous charge-emission rate r_{-0} obtained from an initial-slope analysis of the ΔC^- transient.

the hydrogen-related donor level, without ion implantation, for investigation with conventional DLTS. The procedure involves first releasing hydrogen from PH complexes in the depletion layer and then immediately quenching the diode to a low temperature at which the isolated hydrogen is effectively immobilized at an interstitial lattice site, in preparation for conventional DLTS.

DLTS spectra are shown in Fig. 7 for a diode after the minority-carrier injection (MC) and quenching procedure. The quenching procedure was implemented as follows: with the diode reverse biased at 20 V and held at 240 K, holes where injected into the depletion layer. While continuously injecting holes, the diode was rapidly cooled to below 100 K. In the absence of the hole injection pulse no DLTS signal was detectable on the indicated scale of sensitivity. The double-correlation technique[31] was used to define a spatial observation window bound by depletion depths at 0.6 and 0.9 μm. Spectra are shown for two different reverse biases V_R that produced different average electric fields in the observation window. With each spectrum are listed the peak temperature T_p and the measured activation energy for thermal emission of electrons.

The DLTS spectra in Fig. 7 clearly demonstrate that the thermal emission rate depends on V_R. This indicates a Poole-Frenkel effect,[20] that is, a Coulomb attraction between the hydrogen and the emitted electron. This qualitative feature establishes the donorlike nature of the defect, and indicates the need for a correction to obtain the zero-field values of the emission rate and its activation energy.[32] The authors of Ref. 21 did not present their raw DLTS data for the $E3'$ center, but quoted an activation energy of 0.16 ± 0.01 eV after using a formula due to Hartke[33] to correct their measured emission rates to what they would be in zero field. When we use the Hartke correction similarly on our data, we find two slightly different Arrhenius lines (which should be the same if the Hartke formula were correct), with activation slopes of 0.166 eV for data taken at 4.1-V bias and 0.145 eV from the data at 8.5 V. Thus, it seems that our measurements are consistent with those of Ref. 21. However, there is a modest uncertainty regarding the correct magnitude of the Poole-Frenkel correction: Hartke's model is surely incorrect both at low fields F, where the departure of the correction factor from unity should be $O(F^2)$ instead of $O(F^{1/2})$, and at high fields, where escape by tunneling will eventually dominate over barrier surmounting. Fortunately, the correction is probably small at our lowest field (about 2.6×10^4 V/cm), and since one can reasonably expect the zero-field activation energy to be greater than the Arrhenius slope for the uncorrected escape rates at this field (0.159 eV), it is not unreasonable to accept for the zero-field ionization energy the value 0.16 ± 0.01 eV proposed in Ref. 21. Moreover, the same 0.16 eV was also obtained for the binding energy of an electron to H^+ in a study of the temperature dependence of the H^0:H^+ concentration ratio.[23] Of course, the energies should not be quite the same for the ^{1}H of Refs. 21 and 23 and the ^{2}H of our measurement.

C. Electron-flooding pulse

The addition of an electron-flooding pulse immediately after the hole-injection pulse has a dramatic effect on the capacitance transient, as illustrated in Fig. 8. The top curve arises from the generation and sweep-out of H^+ as described

in Sec. V A. The bottom transient was produced by the addition of an electron-flooding pulse that was applied to the diode for a duration of 10 ms at the end of the hole-injection pulse. This transient begins with a magnitude near zero, ΔC_0^-, and increases with an initial relaxation time τ_- before rolling over and decreasing at long times until reaching a new steady-state value ΔC_{SS}^-. The more complex structure of the ΔC^- curve indicates a richer set of processes than are involved in ΔC^+.

The most striking feature in Fig. 8 is that ΔC, which increases to ΔC_0^+ after the hole-injection pulse, returns nearly to its pre-hole-injection value (i.e., $\Delta C_0^- \approx 0$) after the electron-flooding pulse. The hole pulse creates new donors (P^+) and monatomic hydrogen. Since the electrons supplied by the flooding pulse do not alter the charge state of P^+ and there is not time for appreciable recombination, it must be concluded that the flooding pulse converts enough monatomic hydrogen to H^- to nearly cancel the effect of all the newly created P^+. The ΔC^- transient arises from electron emission, recapture of H^- by P^+, and H migration. The fact that nearly all of the monatomic hydrogen remains as H^- during the zero-bias condition was exploited to determine the diffusivity of H^- in Si near room temperature, as discussed in Sec. V E.

The inset in Fig. 8 shows an Arrhenius plot of the spontaneous emission time $\tau_{-0}(\equiv 1/r_{-0})$ obtained from the initial slope of ΔC^- after correction for sweep out, as described below in Sec. VI A. The T^2 correction arises from the known temperature dependences of the thermal velocity and effective density of states in the prefactor of τ_{-0}.

D. Delayed electron flooding pulse

We have pointed out above that the factor of 2 ratio between the initial and steady-state values of the capacitance change in Fig. 6 (ΔC_0^+ and ΔC_{SS}^+, respectively) agrees nicely with the "pure-H^+ sweep-out" model of Sec. V A. The assumptions of this model—that only H^+ and P^+ contribute to the space-charge transient and that there is no repassivation of P^+ in the depletion region—can be justified by the positions we find for the donor and acceptor levels of hydrogen. However, it is worth noting that a slight modification of the experiment we have just described gives already further support for these assumptions. The modification utilizes a *delayed* electron-flooding pulse. Results are shown in Fig. 9 for the effect on the ΔC^+ transient of a flooding pulse (of 10 ms duration) that is delayed by 3 s after the hole-injection pulse. With the delay time denoted as t_d, the magnitudes of ΔC^+ immediately before and after the delayed pulse, measured relative to $\langle \Delta C_{SS}^+ \rangle$, are labeled ΔC_d^+ $[\equiv \Delta C^+(t_d^-)]$ and ΔC_d^- $[\equiv \Delta C^+(t_d^+)]$, respectively. The magnitude $\langle \Delta C_{SS}^+ \rangle$ is the estimated steady-state capacitance that would have been achieved by $\Delta C^+(t)$ if its evolution had not been interrupted by the delayed pulse.

The pure-H^+ sweep-out model explains the behavior shown in Fig. 9. By Eq. (A3) of Appendix A, all the ΔC's are proportional to the spatial (x) moments of the corresponding charge distributions, that is, to values of the integral in the numerator of Eq. (A3). The moment $M(\Delta P^+)$ of the P^+ newly created by the hole pulse is independent of time and proportional to $\langle \Delta C_{SS}^+ \rangle$. Expressed in terms of moments

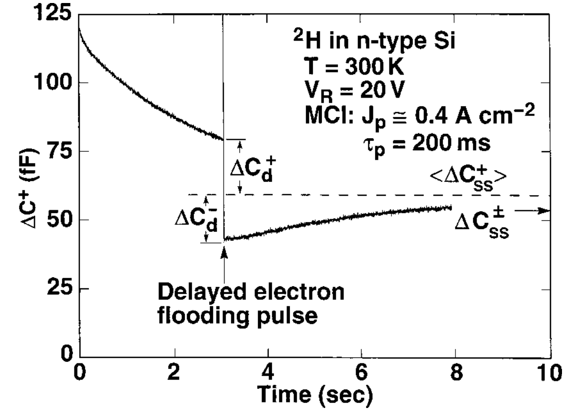

FIG. 9. Effect of a delayed electron flooding pulse on the ΔC^+ transient in Si at 300 K with a delay of 3 s. The quantity $\Delta C_{SS}^{\pm}$ is the measured steady-state capacitance, and the dashed line labeled $\langle \Delta C_{SS}^+ \rangle$ is the estimated steady-state capacitance that would be obtained in the absence of the delayed pulse.

$$\Delta C_d^+(t_d^-) \propto M(\Delta P^+) + M(H^+, t_d^-) \quad (8)$$

while

$$\Delta C_d^+(t_d^+) \propto M(\Delta P^+) - M_>(H^+, t_d^-) + M_<(H^+, t_d^-), \quad (9)$$

where we have separated $M(H^+, t_d^-)$ into a sum of a contribution $M_>$ from the spatial interval between the zero-bias depletion depth x_0 and the full-bias depletion depth W, and a contribution $M_<$ for the interval $x < x_0$. The flooding pulse changes the H^+ in $M_>$ to H^-, hence the negative sign in Eq. (9), but leaves the H^+ in $M_<$ unchanged. Thus, we expect the difference $\Delta C_d^+ - \langle \Delta C_{SS}^+ \rangle$ to be slightly greater than the difference $\langle \Delta C_{SS}^+ \rangle - \Delta C_d^-$, since the small quantity $M_<(H^+, t_d^-)$ increases the former and decreases the latter.

The special value of the delayed-flooding-pulse experiment, however, is that it severely limits the range of possible speculations that depart from the pure-H^+ sweep-out model while retaining consistency with the behavior observed (Fig. 6) without the flooding pulse. We shall discuss only one example of such a speculation, one that might be made if one wished to reject the positions adopted in this paper for the donor and acceptor levels of hydrogen and instead adopted the 1990 suggestion[6] that in traversing a depletion region at room temperature hydrogen comes to a steady state (presumably by electron and hole emission) in which it spends most ($\approx$90%) of its time as H^0, much less as H^+, none as H^-. With this speculation one might assume that hole absorption during the hole pulse created practically 100% H^+ at $t=0$, but that most of this converted to H^0 before being swept out. With this assumption plus the assumption of no repassivation of P^+ by H^+ or H^0, one could get agreement with the observation that $\langle \Delta C_{SS}^+ \rangle \approx \frac{1}{2}\Delta C^+(t=0)$. (Otherwise one would have to assume a coincidental cancellation of the effects of

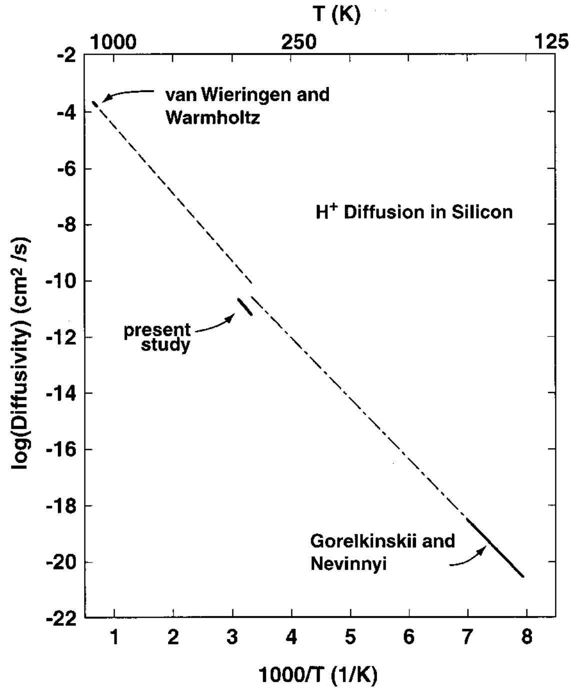

FIG. 10. Arrhenius diagram of measured diffusivities for ${}^1H^+$ in silicon. Results are shown from van Wieringen and Warmholtz (Ref. 2) and Gorelkinskii and Nevinnyi (Ref. 24). In each case the solid segment identifies the measurement range and the dashed portion shows the extrapolation to room temperature, for comparison with results from the present study, Eq. (15).

H^0 at $t=0$ and those of repassivation, which seems unlikely since the factor $\frac{1}{2}$ is observed over the whole temperature range of 260–320 K.) The moment $M(\Delta P^+)$ would then be independent of time up to t_d, and Eq. (8) would again be valid. Now, however, Eq. (9) would be replaced by

$$\Delta C_d^+(t_d^+)\propto M(\Delta P^+)+M_<(H^+,t_d^-)-M_>(H^+,t_d^-)+M(H^0,t_d^-). \qquad (10)$$

Clearly, if t_d is chosen where the second term of Eq. (8) is an appreciable fraction of the first, the alternative model we are here considering will require the last three terms of Eq. (10) to be negative and several times larger than the last term of Eq. (8), so that $\Delta C_d^+(t_d^+)$ falls much farther below $\langle \Delta C_{SS}^+\rangle$ (or $\frac{1}{2}\Delta C_0$) than $\Delta C_d^+(t_d^-)$ lies above it, in extreme contradiction to Fig. 9.

E. Hydrogen diffusivities

The analysis of the capacitance transients, to be presented in the next section, requires the diffusivities of H^+ and H^- as parameters for the quantitative determination of ε_A. Available data on these diffusivities are discussed in this section and summarized in Figs. 10 and 11.

The classic study of hydrogen diffusion in silicon was published by van Wieringen and Warmholtz in 1956.[2] From measurements of hydrogen permeation through silicon at high temperatures (1092–1200 °C), they determined the following Arrhenius dependences for the diffusivity D (Ref. 1, Sec. III.2a):

$$D=9.67\times10^{-3}\exp(-0.48\ \text{eV}/kT)\ \text{cm}^2/\text{s}, \qquad (11)$$

where k is Boltzmann's constant and T is absolute temperature, and the activation energy was estimated to be accurate to 10%. Further, from the square-root dependence of the permeation rate on H_2 pressure, they concluded that hydrogen diffuses predominantly as a monatomic species.

While the measurement was a major experimental achievement that has never been duplicated in silicon, what was not considered in this early study was the possibility that the monatomic hydrogen was in other than a neutral charge state. From the now-known amphoteric properties of isolated hydrogen in silicon, particularly the location of the donor level along with the negative-U character of hydrogen, it can be concluded that the diffusivity determined by van Wierin-

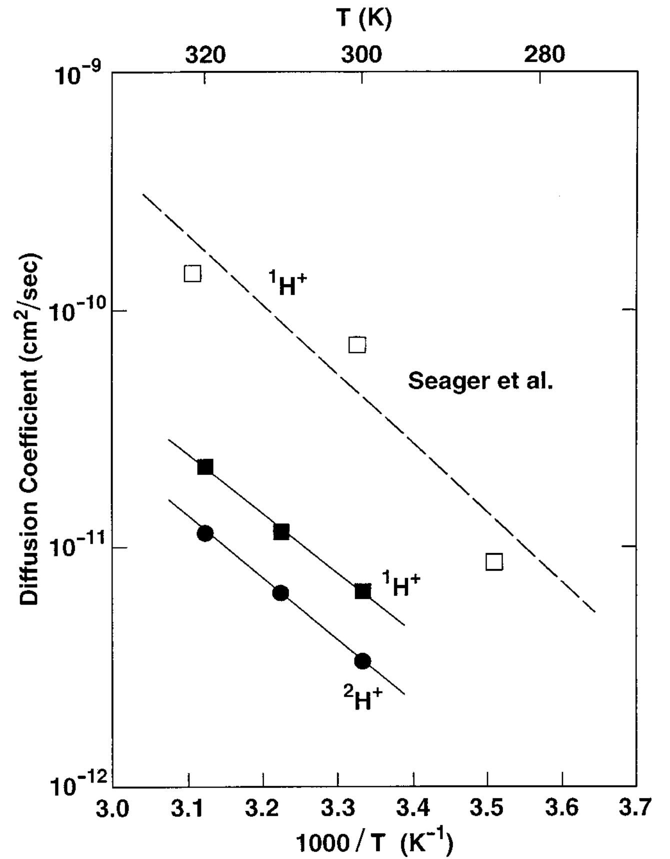

FIG. 11. Comparison of measured diffusion coefficients D_+ of ${}^1H^+$ and ${}^2H^+$ near room temperature. Black circles and squares: values obtained for ${}^2H^+$ and ${}^1H^+$, respectively, by fitting of $\Delta C^+(t)$ curves like that of Fig. 6. Open squares and dashed Arrhenius line: values inferred for $D_+({}^1H^+)$ in 1990 (Ref. 6) from capacitance-voltage measurements of migration of protons implanted into p-type Si at low voltage, using the assumption that a fraction $Q=0.1$ of the migrating hydrogen was H^+ and the rest H^0. As explained in the text, replacement of this assumption by $Q=1.0$ to accord with recent knowledge would bring the results of Ref. 6 into approximate agreement with the present study.

gen and Warmholtz relates predominantly to H^+, rather than to H^0, since at their elevated measurement temperatures ($\geqslant$1092 °C) the material was intrinsic, so that the Fermi level was substantially below $\langle \varepsilon \rangle$. Consequently, Eq. (11) is shown in Fig. 10 as the diffusivity measured by van Wieringen and Warmoltz of H^+, with the solid line indicating the range of measured temperatures and the dashed portion the extrapolation to room temperature.

The observation by Gorelkinskii and Nevinnyi[24] of reorientation of H^+ (AA9 centers) in a uniaxial stress field along [110] and of its recovery gives a clear measure of the hopping time τ_{hop} of H^+ between nearest-neighbor BC sites and therefore of its diffusivity. At not too high temperatures, diffusion of H^+ takes place purely by a random sequence of such hops, for which

$$D_+ = (\text{hop length})^2/(6\tau_{hop}). \tag{12}$$

Although not noted by Gorelkinskii and Nevinnyi, τ_{hop} differs slightly from their measured reorientation time τ:

$$1/\tau = 2F/\tau_{hop}, \tag{13}$$

where F is the fraction of all possible hops that change the orientation of the Si—Si bond in which an H^+ is sitting from being perpendicular to the stress axis to nonperpendicular, or vice versa. Due to the crystallographic inequivalence of the six adjacent BC sites to which an H^+ can hop in a [110]-directed stress field, $F = \frac{2}{3}$. Hence, from Eqs. (12) and (13) and the τ measured by Gorelkinskii and Nevinnyi, the diffusion coefficient is

$$D_+ = 4.24\times 10^{-4} \exp[-0.43 \pm 0.02 \ \text{eV}/kT] \quad \text{cm}^2/\text{s}, \tag{14}$$

for measurements in the range 126–143 K. These results are also plotted in Fig. 10 with the solid segment identifying the measurement range and the dashed portion of the line showing the extrapolation to room temperature.

The capacitance-transient techniques described in previous sections provide an independent means to measure the diffusivity of H^+, which unlike the two determinations just described is applicable near room temperature. In the pure H^+ sweep-out model for the ΔC^+ transient in Fig. 6, all the hydrogen is initially H^+ and gets swept out of the depletion layer by the applied electric field without changing appreciably into H^0 or H^-. The characteristic decay time of $\Delta C^+(t)$ relates to the mobility H^+ and, from the Einstein relation, to the diffusivity. Numerical simulation of the sweep-out kinetics, which incorporated the initial distribution of space charge from C-V data, was used to reproduce experimental ΔC^+ transients over a range of temperatures, with the decay time as fitting parameter. The resultant diffusivities for $^1H^+$ and $^2H^+$ are shown in Fig. 11. They are fitted by[34]

$$D_+(^1H^+) \cong 1.45\times 10^{-3} \exp(-0.497/kT) \ \text{cm}^2/\text{s}, \tag{15}$$

$$D_+(^2H^+) \cong 1.44\times 10^{-3} \exp(-0.504/kT) \ \text{cm}^2/\text{s}, \tag{16}$$

At room temperature the ratio of these diffusivities is $D_+(^1H^+)/D_+(^2H^+) \cong 1.9$.

Also shown in Fig. 11 are values inferred for $D_+(^1H^+)$ from Seager and co-workers[6] over 10 years ago by an analysis of migration of protons implanted at low energy into p-type silicon diodes under reverse bias. In an attempt to account for some puzzling features in migration experiments at zero bias, they were led to assume that in all cases their migrating hydrogen was H^+ only about a tenth of the time ($Q = 0.1$ in their analysis), and H^0 the rest of the time. Though this was conceivable then, we now know that all of the migrating hydrogen must have been H^+. Changing Q to 1.0 removes most of the discrepancy between this older work and our present results.

Our diffusivity for $^1H^+$ is also shown in Fig. 10 for comparison with the extrapolated high-temperature results from van Wieringen and Warmholtz[2] and the extrapolated low-temperature results from Gorelkinskii and Nevinnyi.[24] The agreement among the three sets of data, and especially between our results and those of Gorelkinskii and Nevinnyi, is impressive. The uncertainties of the Arrhenius slopes are such that a single straight line could easily fit both sets of data within the probable errors. An important conclusion is that tunneling of $^1H^+$ between nearest-neighbor sites, which at low temperatures should eventually dominate over thermally activated over-barrier motion, does not yet do so at 125 K.

The only reported determination of the diffusivity D_- of H^- was obtained with the time-resolved capacitance transient techniques described in previous sections.[8] The estimation of D_- was obtained from the rate of recombination of H^- with P^+ near room temperature. The simple model used for data analysis slightly overestimated the magnitude of the diffusion coefficient and provided a useful upper limit of 0.70 eV for the activation energy, with $D_-(^2H^-, 300\,\text{K}) \cong 3\times 10^{-12}\,\text{cm}^2/\text{s}$.

Our measurements of diffusion for both the positive and negative monatomic species have tacitly assumed that any hydrogen not bound to a phosphorus or to another hydrogen spends most of its time as an isolated monatomic species at a minimum-energy interstitial configuration surrounded by perfect silicon. A similar assumption is used in our determination of the position of the hydrogen acceptor level in Sec. VI B below, and we shall cite evidence there in support of this assumption.

VI. ANALYSIS

A. Initial slope analysis of electron emission

The lower curve ΔC^- in Fig. 8 results from the addition of an electron flooding pulse immediately after the hole injection pulse, which converts the newly released H^+ to H^-. The diode capacitance $\Delta C^-(t)$ rises with time because the initial slope of ΔC^-, $[d\Delta C^-(t)/dt]_{t=0}$, is made up of two competing contributions, drift of H^- (and of a small amount of H^+ present inside the zero-bias depletion layer), which gives a negative term, and charge change $H^- \rightarrow H^0 \rightarrow H^+$, which gives a positive term. Figure 8 shows that the latter term dominates. Each of the terms can be directly related to other observable parameters, to yield an expression from

which the spontaneous electron emission time τ_{-0} ($\equiv 1/r_{-0}$) can be determined. The analysis follows.

The small ionization energy of the hydrogen donor level ensures that near room temperature the second step, $H^0 \rightarrow H^+ + e^-$, in the spontaneous conversion of H^- to H^+ occurs practically instantaneously compared with the slower first step $H^- \rightarrow H^0 + e^-$ (cf. the more detailed discussion in Sec. X below). So we can write, with subscript "0" for $t=0$,

$$[d\Delta C^-/dt]_{t=0} = [d\Delta C^-/dt]_{0,\text{charge change}} + [d\Delta C^-/dt]_{0,\text{drift}} = (1/\tau_{-0})[\Delta C^+(0) - \Delta C^-(0)] + [d\Delta C^-/dt]_{0,\text{drift}}. \quad (17)$$

Here $[d\Delta C^-/dt]_{0,\text{drift}}$ is an integral of contributions from all depth intervals dx from the surface, $x=0$, to the reverse-bias depletion depth. The contribution from any dx in the zero-bias depletion region will be the same as the contribution from this region to $[d\Delta C^+/dt]_{0,\text{drift}}$, since the hydrogen here persists as H^+ after the short flooding pulse, and $E(x)$ at $t=0$ is not changed. At greater depths H^+ is changed to H^-, but if D_- happens to be the same as D_+, its drift velocity in the electric field will be exactly equal and opposite to that of H^+ at $t=0$ without a flooding pulse, hence the region's contribution to $[d\Delta C^+/dt]_{0,\text{drift}}$ will again be the same as that to $[d\Delta C^-/dt]_{0,\text{drift}}$. So for $D_- = D_+$ we can set

$$[d\Delta C^-/dt]_{0,\text{drift}} = [d\Delta C^+/dt]_{0,\text{drift}} = [d\Delta C^+/dt]_0, \quad (18)$$

which is measurable.

By how much does Eq. (18) need to be corrected when $D_- \neq D_+$? The answer depends not only on the ratio D_-/D_+, but also on the x dependence of the concentrations of newly created monatomic H and of *total* donors (P^+ in our case). A straightforward calculation, especially simple when both of the latter concentrations are uniform, gives

$$[d\Delta C^-/dt]_{0,\text{drift}} = [d\Delta C^+/dt]_{0,\text{drift}}[A + (D_-/D_+)(1-A)], \quad (19)$$

where A is close to $\frac{1}{2}$ when the concentrations are uniform and the zero-bias and reverse-bias depletion depths are those appropriate to the experiment of Fig. 8. From Eqs. (17) and (19) we obtain

$$\tau_{-0} = [\Delta C^+(0) - \Delta C^-(0)]/\{[d\Delta C^-/dt]_0 - [d\Delta C^+/dt]_0[A + (D_-/D_+)(1-A)]\}. \quad (20)$$

By our present measurements (Sec. V E above), D_- and D_+ are almost equal at 310 K, though our estimate of D_- is rather rough. For the values of τ_{-0} presented in Fig. 8 and for the determination of ε_A in Sec. VI B below we have used Eq. (20) with $A=\frac{1}{2}$ and the values obtained in Sec. V E for $D_+(^2\text{H},T)$ and $D_-(^2\text{H},T)$. The sensitivity of the value of Eq. (20) to the assumed values of D_-/D_+ and A is only modest: for example, for the data of Fig. 8, changing D_-/D_+ to $\frac{1}{2}$ or 2 while keeping $A=\frac{1}{2}$ would change τ_{-0} by $+14\%$ or -11%, respectively, while changing A to anything while keeping $D_- = D_+$ would not change τ_{-0} at all; changing both parameters by factors of 2 up or down could change τ_{-0} by at most $+22\%$ or -27%. To change ε_A by 0.01 eV would require a change of $+45\%$ or -31% in τ_{-0}.

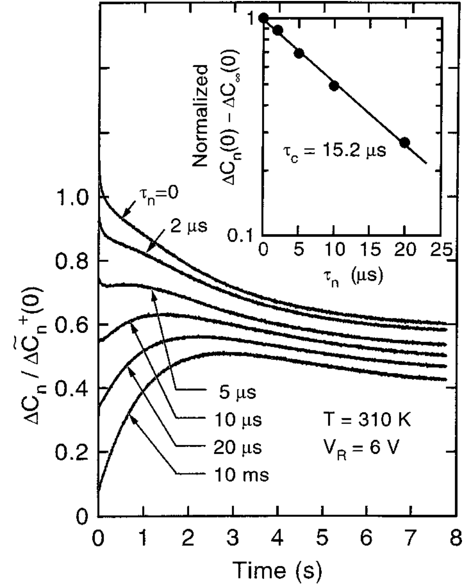

FIG. 12. Capacitance transients $\Delta C_n(t)$ recorded after the following sequence of operations: dissociation of PH complexes by a hole pulse at a reverse bias of 20 V, immediate reduction (i.e., after 10 ms) of the bias to zero for a duration τ_n, and imposition of a new reverse bias of 6 V. The inset shows the exponential decay of the normalized values of $\Delta C_n(0)$ toward their long-time $\Delta C_\infty(0)$ ($\tau_n = 10$ ms) limit, which yields the electron capture time τ_C.

B. Filling-pulse width dependence and location of the acceptor level

The rate r_{0-}, or equivalently the rate of Eq. (5a), was determined by studying the amount of conversion of H^+ to H^- due to zero-bias pulses of very short duration τ_n. A set of such capacitance transients $\Delta C_n(t)$ recorded at 310 K is presented in Fig. 12. The ΔC values for each τ_n are normalized by a value $\Delta C_n^+(0)$, which for $\tau_n=0$ represents an extrapolation of the observed curve to $t=0$ to eliminate the effect of a small initial thermal transient (cf. Sec. IV C), and which for the other τ_n's represents this extrapolation plus normalization to the actual number of hydrogen atoms released in the nth run. The latter normalization was enabled by inserting a short (10 msec) delay between the hole pulse and the zero-bias pulse. The inset shows the exponential decay of the normalized values of $\Delta C_n(0)$ toward their long-time $\Delta C_\infty(0)$ (i.e., $\tau_n = 10$ msec) limit, which yields the electron capture time τ_c for the process in Eq. (2a).

To determine the rate r_{0-} at which H^0 captures an electron during a flooding pulse, the location of the Fermi level must be considered. If $\varepsilon_F \leqslant \varepsilon_D$, the rapid equilibration of H^0 and H^+ implies that during the flooding only a fraction

$$F_0 = \{\tfrac{1}{2}\exp[(\varepsilon_D - \varepsilon_F)/kT] + 1\}^{-1} \quad (21)$$

of the hydrogen not yet converted to H^- will at any instant be H^0, where k is Boltzmann's constant. Thus, the r_{0-} to be used in Eq. (4) is $(F_0 \tau_c)^{-1}$.

While for $F_0 \approx 1$ the calculated ε_A does not depend on ε_D, in the opposite limit of $F_0 \ll 1$ it is $\varepsilon_A + \varepsilon_D$ that becomes independent of ε_D. For the measurement conditions of Fig. 8 (i.e., average electron concentration of $5.6\times 10^{15}\,\mathrm{cm}^{-3}$ and $T=310\,\mathrm{K}$) and the value for ε_D of $\sim$0.40 eV above midgap (cf. Sec. V B), F_0 is 0.10 and ε_A is $\sim$0.07 eV below midgap. (These figures differ slightly from those of Ref. 27, mainly because of the higher assumed position of ε_D.)

As we noted earlier, the validity of our determinations of diffusion coefficients and our location of the acceptor level depends on our being able to assume that nearly all the hydrogen released into the depletion region of a diode by hole injection drifts out of the depletion region during the capacitance transient, if the reverse bias is maintained. Our repeated observance of values close to $\frac{1}{2}$ for the ratio $\Delta C_{\mathrm{ss}}^+/\Delta C_0^+$ in transients like that of Fig. 6 is consistent with this assumption, but would be inconsistent with trapping of any appreciable fraction of the H^+ by association with any neutral center I to form a stable complex HI^+ or with an initially negative center A^- to form a stable neutral complex HA. The only appreciable trapping that could be consistent with the ratio $\frac{1}{2}$ would be combination of H^+ with I^0 accompanied by emission of a hole to yield a neutral complex. But for such capture to occur in the short time of the experiment, with the small capture radius expected for a neutral center, would probably require a rather large density of I^0 centers ($\geq 10^{17}\,\mathrm{cm}^{-3}$), and in the absence of other evidence for such, we feel that it is unlikely.

In the analysis of the present section, which makes use of the initial slope of the curve $\Delta C^-(t)$ measured at reverse bias after the H^+ has been converted to H^- by a (usually short) exposure to zero bias, we have assumed the H^- to undergo drift, diffusion, and capture by P^+, but no other trapping. This assumption is consistent with the observation, made on several samples, that prolongation of the zero-bias period for a time much longer than the H^--P^+ recombination time gives a $\Delta C^-(t)$ curve that is horizontal at a height of the order of $0.1\Delta C_0^+$, as would be expected if nearly all the H^- had recombined with P^+ before diffusively migrating in depth by more than a small fraction of the thickness of the reverse-bias depletion region. This agreement would be spoiled if a sizable fraction of the H^- formed stable neutral complexes by combining with some foreign center and emitting an electron. However, combining with a positive center I^+ other than P^+ to form a stable neutral HI complex, or with a neutral center I^0 to form a stable complex HI^-, could be perfectly consistent with the observed small $\Delta C^+(t)$ after a long zero-bias period. The I^+ scenario would not invalidate our determination of D_- or that of ε_A. The I^0 scenario would affect our D_- if its probability were comparable with that of $H^- + P^+ \rightarrow PH$, but because of the expected lower capture radius for I^0 than for P^+, this would require an unreasonably high concentration for I^0. As for our determination of ε_A, the I^0 scenario would modify the inferred rate of the thermally driven reaction $H^- \rightarrow H^0 + e^-$ merely by modestly increasing the value of D_- to be used in calculating the contribution of H^- drift to $[d\Delta C^-(t)/dt]_{t=0}$; the charge change rate ($H^- \rightarrow H^+ + 2e^-$) required to outweigh this drift contribution by enough to account for the observed value of $[d\Delta C^-(t)/dt]_{t=0}$ would then have to be increased by a fractional amount rather less than the fractional increase in D_-. [Since the derivative has to be evaluated using a finite time duration t_{av} of the $C^-(t)$ curve, one should in principle allow for the small effect of PH and HI^- complexes on the average derivative, an effect whose relative order is roughly the ratio of t_{av} to the lifetime of H^- with respect to complex formation, a ratio so small for PH that we have already neglected it.]

VII. COMPUTATIONAL THEORY

Our analysis of the experimental results is based on the following two assumptions: (i) both reactions in Eqs. (5) proceed via an essentially equilibrium state of H^0 and (ii) the rates of $H^0 \leftrightarrow H^+ + e^-$ are fast compared with the corresponding rates for $H^- \leftrightarrow H^0 + e^-$. Support for these assumptions is provided by calculations of total energy as a function of lattice configuration, with a first-principles density-functional pseudopotential technique previously described.[10,11,27] These calculations yield energy surfaces for hydrogen in the positive, neutral, and negative charge states, that is, the energy of the system as a function of the coordinates of the hydrogen atom, with the Si atoms fully relaxed for each hydrogen position. As discussed in Sec. II A, energy differences between different charge states depend on the position of the Fermi level. In the following discussion, we assume the Fermi level to be located at the bottom of the conduction band. Figure 2 shows the values of the energy differences between H^+ at BC, H^0 at BC, and H^- at T_d for this choice of ε_F, that is, for the minimum-energy positions of the H atom in each charge state. The complete total-energy surfaces allow us to investigate the energy differences between the charge states for *any* position of the H atom. At each hydrogen position we can identify which charge state has the lowest energy. We can therefore also identify at which point in space the hydrogen will change charge state, as it moves through the crystal. A graphical representation of these energy differences as a function of the three spatial coordinates of the hydrogen atom is cumbersome. However, inspection of the full-energy surfaces has allowed us to identify a path between the BC and T_d sites that captures the essence of the energetics. This path is shown in the inset of Fig. 13. The path has the property that for the lowest-energy charge state, the energy is very nearly a minimum with respect to displacements of the hydrogen normal to the path. Figure 13 can therefore be interpreted as a configuration-coordinate diagram.

Our choice for the Fermi energy, $\varepsilon_F = \varepsilon_C$, corresponds to plotting the energy of H^-, H^0 plus one electron at the bottom of the conduction band, and H^+ plus two such electrons. The energies shown in Fig. 13 have been taken directly from the density-functional calculations, with no correction for the band-gap error. However, the simple correction scheme mentioned in Sec. II A and used in Fig. 2, in which all defect levels are shifted rigidly upwards along with the conduction

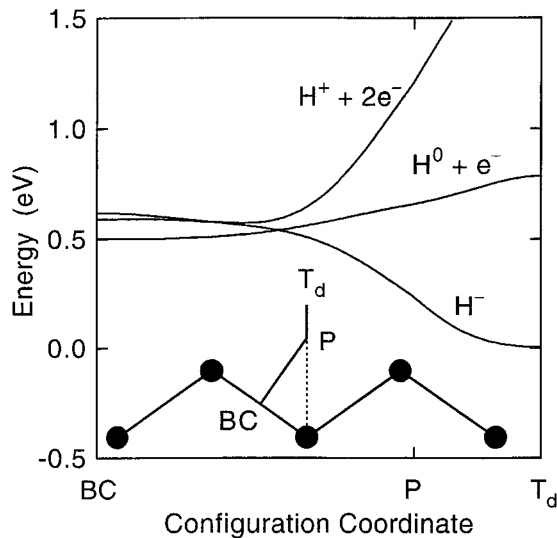

FIG. 13. Variation of the calculated energies of H^+, H^0, and H^- in the silicon lattice, as a function of atomic position along the path shown in the inset. This path extends from the BC site to the T_d site in the (110) plane. For each H position the Si atoms are optimally relaxed. The zero of energy has been chosen to correspond to the energy of H^- at T_d, and energy differences between the charge states are shown for $\varepsilon_F = \varepsilon_C$; the energies for H^0 and H^+ therefore include those of one or two electrons at the bottom of the conduction band.

band, does not affect the position of transition levels with respect to the conduction band, and hence would not affect the energy differences depicted in Fig. 13. Other correction schemes might shift the relative heights of the three curves, but would probably have much less effect on their individual shapes.

Of particular interest to the present work is the question whether the energy surface for H^0 includes any metastable states. If no such metastable states exist, then a transition from H^- to H^0 at some nonequilibrium lattice configuration will cause the system to coast downhill to the global minimum at BC. We have therefore investigated the energy surface for H^0 in greater detail than in our original studies.[10] In particular, we have explored configurations in which H is located in an antibonding (AB) position with respect to a S—Si bond, with possible formation of a bond between the H and the Si atoms, and partial breaking of the Si—Si bond. This AB site was found to be a local minimum in cluster calculations by Deák, Snyder, and Corbett[35] and Maric and co-workers.[36] Cluster calculations by Estreicher[37] produced a local minimum at T_d, but not at the AB site. Our detailed exploration of such configurations has produced no metastable minima in the energy surface for H^0, to within the numerical accuracy of the calculations (i.e., a few 0.01 eV). Even if there should turn out to be a metastable site for H^0, it seems unlikely that the barrier against escape to BC could be high enough to delay such escape by more than nanoseconds at room temperature. Thus, transfer to near BC should happen quickly, before there is time for a fluctuation to the higher energy necessary to reach the H^+ curve. Hence assumption (i) seems likely to be the case for the electron-emitting transitions. For the electron-absorbing ones, $H^+ + e^-$ will generate H^0 in a configuration that needs only a small downhill readjustment to reach that of ground-state H^0, so assumption (ii) is justifiable as well.

VIII. APPLICATIONS OF THE NEGATIVE-*U* PICTURE

The preceding sections have presented a fairly detailed picture of the stationary states of monatomic hydrogen in silicon and of the rates of charge-change reactions between them, a picture derived in part from our experiments and from those of Refs. 21, 22, and 23, and in part from first-principles theoretical calculations; the principal conclusions are summarized in Sec. XIV. As we shall now show, this "negative-*U* picture" provides an extremely useful framework for understanding a number of facts in the behavior of silicon-hydrogen that have been observed but not previously explained, and for narrowing the range of speculation about the mechanisms of other phenomena. Much of the quantitative reasoning in the following sections involves use of equations relating the concentrations of the various monatomic species and diatomic complexes when all these are locally in mutual thermodynamic equilibrium with each other and with the electronic distribution, though occasionally we may wish to consider nonequilibrium situations (e.g., the depletion region of a reverse-biased diode). The problems we shall consider will all involve a single type of dopant, usually a shallow donor which for definiteness we shall call phosphorus, monatomic hydrogen, complexes of dopant with hydrogen (PH for definiteness), and a single type of diatomic hydrogen complex which we label H_2 and assume to have the most stable configuration for a diatomic complex, although there is still some uncertainty as to the details of this configuration.[38] If we assume thermal equilibrium, but do not yet impose charge neutrality, the concentrations of all these species at any given location in space are all determined in terms of three independent variables, which we are free to choose in any of a variety of ways. We have derived and tabulated expressions for all the various concentrations in Appendix B, using as independent variables the particularly convenient set consisting of the concentrations n_{P} of shallow-donor atoms and $n_{\mathrm{P}+}$ of unpassivated ones, and, for cases without a charge-neutrality constraint, the Fermi level ε_F. Appendix B also gives brief descriptions of various simplifying approximations that can be used in the equations, and of some of the numerical values that will be used in the evaluations to be given below.

The effects that we have chosen for discussion in the remainder of the paper are the fact that more intense hydrogenation is required to passivate shallow donors in silicon than to passivate shallow acceptors (Sec. IX); the fact that despite similar dissociation energies donor-hydrogen complexes are much more easily dissociated by minority carriers than acceptor-donor complexes (Sec. X); the fact that hydrogen dissolved in silicon at incandescent temperature will transfer at moderate temperatures to acceptors in *p*-type Si much more easily than to donors in *n*-type Si (Sec. XI); evidence that the binding energy of H_2 with respect to dissociation is quite high, of the order of 1.75 eV (Sec. XII); and evidence

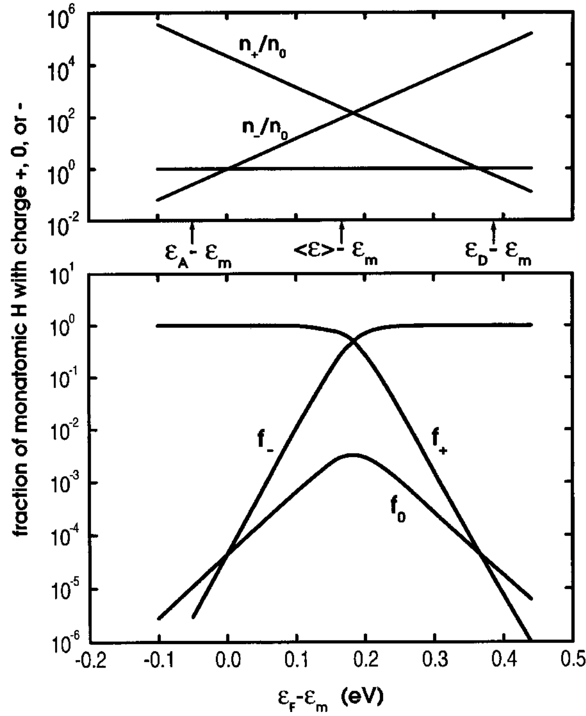

FIG. 14. Relative concentrations, in equilibrium, of the different charge states of monatomic hydrogen as functions of the position of the Fermi level in the gap. Top diagram: values of n_+/n_0 and n_-/n_0 at 150 °C. Lower diagram: same data plotted as fractions of total hydrogen $n_{\rm tot}$ in each of the three charge states.

that the diffusive migration of H_2, recently measured in the range 125–200 °C, occurs by migration of an undissociated pair (Sec. XIII).

All these topics can be understood in terms of reactions involving monatomic hydrogen, with mass-action equations involving the concentrations n_+, n_0, n_- of the various charge states, whose ratios in electronic equilibrium are related by Eqs. (B2) and (B3) of Appendix B, and depend on the Fermi energy ε_F, the donor and acceptor levels (at $T=0$) ε_D and ε_A, respectively, the statistical weights (number of possible configurations in a unit cell) ν_i for each species i, and the vibrational partition functions Z_i associated with each species (which approach unity as $T\to 0$). When $U \equiv \varepsilon_A - \varepsilon_D$ is negative, as it is for hydrogen, these equations give abundance ratios that vary with ε_F as shown in the upper part of Fig. 14. Replotting the curves to show the fractions of total monatomic hydrogen in each of the charge states gives the curves in the lower part of the figure. Note that the concentration of H^0 is always much smaller than that of the more abundant of H^+ and H^-. Since the mean energy $\langle\varepsilon\rangle$ of ε_D and ε_A is well above the midgap level ε_m, hydrogen introduced into silicon at very high temperatures (e.g., as in the classic study by van Wieringen and Warmholtz,[2] where intrinsic conditions prevail), probably consists predominantly of H^+ at these temperatures, although the unknown temperature dependence of the Z_i makes it hard to predict the charge-state abundances precisely.

IX. NEUTRALIZATION EQUILIBRIA

It has long been known that while it is easy with any of several hydrogenation techniques[40] to passivate a large proportion of the near-surface shallow acceptors in p-type silicon, similar treatment of comparably doped n-type silicon passivates far fewer of the shallow donors. A superficial interpretation of this fact would be to conclude that the binding energy of hydrogen to donors is much less than that to acceptors. But this is not true, at least if "binding energy" is defined as the minimum energy to dissociate the bound complex to widely separated monatomic species. A crude indication that the binding energies of PH and BH are comparable is provided by the activation energies of their dissociation rates in biased diodes, for which 1.18 eV (PH near 65 °C) (Ref. 7) and 1.28 eV (BH over a similar but wider range[41]) have been reported. These activation energies of course involve the temperature dependence of the diffusion coefficient D_+ or D_- and that of the Coulomb capture radius R_C^0, as well as the binding energy $\Delta\varepsilon$. One of the possible ways of extracting the latter quantity from observed dissociation rates is discussed in Appendix B, and, with inclusion of a correction for the effect of the high field in the diode on the dissociation rate, yields the values $\Delta\varepsilon_{\rm PH}\approx 0.71$ eV and $\Delta\varepsilon_{\rm BH}\approx 0.77$ eV, in zero field. While either of these may well be in error by several hundredths of an eV, we shall adopt them for the calculations to be displayed here.

The main source of the difference in ease of passivation between n-type and p-type silicon becomes obvious[42] when one looks at the mass-action equations for equilibrium of P^+ and PH [Eq. (B4)]

$$n_{\rm PH} = K_{\rm PH} n_{\rm P^+} n_- \tag{22}$$

and for that of B^- and BH, obtained similarly,

$$n_{\rm BH} = K_{\rm BH} n_{\rm B^-} n_+ , \tag{23}$$

where in the low-temperature approximation Eqs. (B4) and (B17) give

$$K_{\rm PH} = 2\Omega_0 \exp(\Delta\varepsilon_{\rm PH}/kT), \quad K_{\rm BH} = \Omega_0 \exp(\Delta\varepsilon_{\rm BH}/kT). \tag{24}$$

The big difference is that for comparable hydrogenation conditions, the n_+ in p-type material is vastly larger than the n_- in comparably doped n-type material, as we have just shown in Fig. 14. If we express n_- and n_+ in terms of n_0, we can convert Eqs. (22) and (23) into formulas that provide a convenient, quick picture of the dependence of the degree of passivation on concentration of donor or acceptor species ($n_{\rm P}$ or $n_{\rm B}$) and on intensity of hydrogenation (roughly measured by the neutral hydrogen concentration n_0, although there may well be a moderate dependence of the n_0 produced by a given plasma-product exposure on the chemical doping). Thus, Eqs. (B9) and (B10) convert Eq. (22) to

$$n_{\rm PH}/n_{\rm P^+} = (K_{\rm PH}/4n_i)\exp[(\varepsilon_m - \varepsilon_A)/kT](n_0 n_{\rm P^+}), \tag{25}$$

while the p-type analogs of Eqs. (B10) and (B11) convert Eq. (23) to

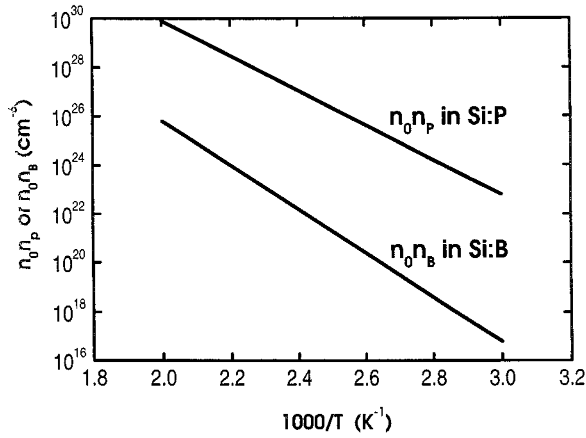

FIG. 15. Doping levels required for 50% passivation of phosphorus-doped n-type silicon or boron-doped p-type silicon, as functions of the reciprocal temperature. To allow for the effect of intensity of hydrogenation the vertical scale represents the product of the dopant density, n_P or n_H, by the concentration n_0 of neutral hydrogen. The degree of passivation increases upward.

$$n_{BH}/n_{B^-} = (K_{BH}/2n_i)\exp[(\varepsilon_D - \varepsilon_m)/kT](n_0 n_{B^-}). \quad (26)$$

Figure 15 gives a numerical picture of the consequences of Eqs. (25) and (26), by plotting the lines, in the space of temperature versus n_0n_P or n_0n_B, across which the passivation of P in Si:P or of B in Si:B passes the 50% level. These are the loci on which the right-hand side of Eq. (25) equals 1 with $n_{P^+} = \frac{1}{2}n_P$, or that of Eq. (26) equal to 1 with $n_{B^-} = \frac{1}{2}n_B$, respectively. The choice of ordinate is natural since n_P or n_B characterizes the choice of material, and since for plasma hydrogenation n_0 is probably, as noted above, mainly determined by the exposure conditions and the nature of the plasma products.

X. MINORITY-CARRIER-ENHANCED DISSOCIATION OF DOPANT-HYDROGEN COMPLEXES

As we have described in Sec. II B, it has been found experimentally that injection of minority holes (h^+) greatly enhances the thermal dissociation of PH complexes in n-type silicon, and we have proposed that this occurs by a thermal fluctuation to P^+ and H^- in close proximity followed by $H^- + h^+ \rightarrow H^0$ and diffusion away of H^0 unhindered by the Coulomb field. It may seem natural to ask whether an analogous dissociation can be produced from say, BH complexes by minority electrons in p-type silicon. Indeed, some observations of forward-biased diodes[43,44] or diodes under illumination[43,45] have been interpreted in terms of augmented BH dissociation. In the two most detailed of such systems,[44,45] published almost simultaneously, similar observations were made, but quite different interpretations were proposed. In both cases it was found that, in the region of a partially passivated Schottky diode beyond the zero-bias depletion depth, introduction of excess minority electrons reduced the concentration of BH complexes, with a corresponding increase of the B^- concentration, as determined by capacitance-voltage profiling. Seager and Anderson[44] concluded that "injection of minority carriers can markedly accelerate the dissociation process" and attributed this acceleration to the analog of the process we have described in Sec. II B, that is, to conversion of a partially dissociated H^+ to H^0 and diffusion of the latter away from the B^-. Such an effect seemed reasonable in 1991, when the location of the H^+:H^0 donor level was not known, but was widely assumed to be near midgap. Zundel and Weber,[45] however, studied the effect of many factors (time, temperature, doping, and light intensity) on the rate of conversion of BH into B^- and "invisible" hydrogen (presumed to be a diatomic species) and concluded that the rate-determining process was the generation of H_2 by encounters of H^0 with H^+, with the concentration of H^0 a small fraction of that of H^+, proportional to the electron concentration: they found no indication of any dependence of the rate of dissociation of BH on electron concentration.

We have looked for dissociation of BH complexes by minority electrons in the depletion region of a reverse biased p-type Schottky diode, using electrons generated by 1.53-eV photons incident on the back side of the wafer, that is, in a procedure exactly analogous to that used in Ref. 17. In comparison with the experiments discussed in the preceding paragraph this has significant advantages: what is measured is the dissociation rate itself, rather than the difference between dissociation and recombination; no correction for diffusion is needed; and the dissociation cross section, or an upper limit for it, can be measured with reasonable accuracy because both the dissociation rate and the electron density can be reasonably well determined. However, it is not possible with our method to measure an electron-stimulated augmentation of the dissociation rate when it is small compared with the rate in the absence of excess electrons. For this reason the maximum temperatures used in the experiments to be reported here were somewhat lower than the maximum reached in Refs. 44 and 45 (145 and 160 °C, respectively).

Our samples were silicon doped with $9\times10^{16}\,\mathrm{cm}^{-3}$ of boron and subsequently passivated by exposure for 30 min at 130 °C to downstream gases from a hydrogen plasma; this reduced the near-surface active acceptor concentration, as revealed by capacitance profiling, to $2.5\times10^{15}\,\mathrm{cm}^{-3}$ at a depth of 0.8 μm and to $1\times10^{16}\,\mathrm{cm}^{-3}$ at a depth of 2 μm. An aluminum Schottky contact was deposited through a shadow mask onto the polished front face and Ohmic contacts were evaporated onto the rear face, in a geometry similar to that of Fig. 4. With a reverse bias applied to the Schottky diode, an opening in the Ohmic contact on the rear face, opposite the Schottky metal, was illuminated with 1.53-eV laser light for various periods of time, same as described for the n-type diodes in Sec. IV B. After each period of illumination the active acceptor distribution in the diode was profiled by measurement of the capacitance-voltage relation. Over the range of conditions we covered, namely, integrated exposures up to 1.3×10^{12} electrons seconds per cm^3 and temperatures up to 320 K, there was no detectable depassivation (i.e., conversion of $\leqslant$2% of the BH to B^-).

The figures just given imply that the cross section for $BH + e^- \rightarrow B^- + H^0$ is less than about $3\times10^{-21}\,\mathrm{cm}^2$ at 300 K. This contrasts with the cross section $1\times10^{-19}\,\mathrm{cm}^2$ measured for $PH + h^+ \rightarrow P^+ + H^0$ in Ref. 17 at 270 K, the temperature at

which the ordinary thermal dissociation rate of PH is about the same as of BH at 300 K. This difference between the two cases is in fact just what one would expect from the nature of the dissociation process and the asymmetry in the positions of the hydrogen donor and acceptor levels in the energy gap. One might at first imagine that dissociation of BH by electrons could occur by a sequence of processes analogous to that described at the beginning of this section for dissociation of PH by holes, that is, $BH \rightarrow B^- + H^+$, $H^+ + e^- \rightarrow H^0$, $H^0 \rightarrow \infty$; this was in fact suggested by Seager and Anderson.[44] But present knowledge about the statistics of the reactions $H^+ + e^- \leftrightarrow H^0$ implies that at room temperature and above the thermal ionization of H^0 is so rapid that it is enormously dominant over the reverse (electron capture) reaction. While the rates will be somewhat different for a hydrogen close to a B^- than for an isolated hydrogen, the fact that the ionization energy is lower in the former case implies that H^+ will be even more dominant. As we shall now argue quantitatively, this means that any H^0 momentarily formed from a partially dissociated BH will revert to H^+ long before it has had time to diffuse an appreciable distance, and the H^+ will be rapidly drawn back to the B^-. Of course, if the electron concentration n_e becomes very high, an appreciable number of H^0 may be converted to H^- before they autoionize, and this could greatly increase the dissociation rate of BH, via a contribution quadratic in n_e. We shall ignore this class of cases, confining attention to effects of first order in n_e. For the PH dissociation, on the other hand, the spontaneous ionization of an H^0 formed near a P^+ will accelerate the dissociation by repulsion of the H^+ from the P^+, even in the linear range.

The spontaneous ionization rate $1/\tau_{0+}$ of H^0 can be estimated by extrapolating the results of low-temperature DLTS measurements on the $E3'$ center, now reliably identified[23] as hydrogen at a bond-center site. These gave an ionization rate of 80.5 s^{-1} at about 73.4 K and an ionization energy of at least 0.16 eV. Extrapolation to 300 K (400 K) gives, very roughly, a spontaneous ionization rate of $1.6\times10^{10}\,s^{-1}$ ($7.4\times10^{10}\,s^{-1}$). Correspondingly, the equilibrium population ratio $[H^0]/[H^+]$ in silicon with 5×10^{15} active acceptors/cm^3 should be $2\exp[(\varepsilon_D-\varepsilon_F)/kT]$, hence at 300 K (400 K) about 1.1×10^{-12} (1.3×10^{-8}). In the presence of a nonequilibrium concentration of minority electrons, the ratio $[H^0]/[H^+]$ will approach equilibrium with the quasi-Fermi-level ε_{Fe} of the electrons, but it will still be $\ll 1$ as long as the electron concentration n_e is well below its value for $\varepsilon_{Fe}=\varepsilon_D$ (i.e., $5\times10^{16}\,cm^{-3}$ at 300 K or $1\times10^{17}\,cm^{-3}$ at 400 K). For lower n_e, the hydrogen will spend much more time as H^+ than as H^0, and unless H_0 is much more mobile than H^+, the small abundance of H^0 cannot contribute much to the overall escape probability.

Although a huge value of D_0/D_+ may seem very implausible, there has never been a measurement of D_0, and there are only one or two observations from which, with plausible assumptions, one may derive crude upper limits for it. So we have examined both the experimental evidence on D_0 (Refs. 24 and 46) and the theoretical kinetics of dissociation with a fluctuating charge state, in an attempt to estimate a rough upper bound on the effective cross section for the dissociation of BH by electrons. The results of these studies, details of which are available[47] but will not be given here, are as follows. First, D_0/D_+ is not likely to be greater than about 10^3 at 400 K, and may perhaps be far below this limit. Second, to first order in the electron concentration, the effect of minority electrons on the dissociation rate $1/\tau_{BH}$ of BH obeys

$$\tau_{BH}^{(0)}/\tau_{BH} \leqslant 1+(D_0/D_+)\exp[(\varepsilon_D-\varepsilon_{Fe})/kT], \qquad (27)$$

where $1/\tau_{BH}^{(0)}$ is the thermal dissociation rate in the absence of electrons and ε_{Fe} is the quasi-Fermi-level of the electrons. The second term on the right of Eq. (27) is quite small for any p-type silicon at $T\sim400$ K.

XI. DOPANT GETTERING OF DIATOMIC HYDROGEN

Recently several papers[48–51] have studied the solubility of hydrogen in silicon at incandescent temperatures by utilizing a very simple means to measure the total amount of hydrogen introduced by high-temperature equilibration of a fairly thick (a new millimeters) silicon sample with hydrogen gas at known pressure. Namely, boron-doped silicon (concentration $n_B=1\times10^{17}\,cm^{-3}$) is hydrogenated thus at high temperature (900–1300 °C) and then quenched to room temperature, preferably with an intermediate anneal of the order of a few hours at around 175 °C.[50,51] At the latter temperature it is found that nearly all the hydrogen (concentration $n_H \leqslant n_B$) settles into BH complexes, whose density can easily be measured by the infrared absorption of their stretching mode. The hydrogen, nearly all monatomic at the highest temperatures, has presumably combined into diatomic H_2 at intermediate temperatures, but by 175 °C the configurational entropy associated with the random positioning of these complexes no longer suffices to overcome the preference of the hydrogen for what is evidently a lower energy state, namely binding to some of the abundant boron ions. The presence of H_2 molecules in the quenched material, before annealing at 175 °C, was detected with vibrational spectroscopy,[52] which revealed a line at 3618 cm^{-1} that has been assigned to the vibrational mode of isolated H_2 molecules.[53,54] Since the dissociation energy of the PH complex is, as we noted in Sec. X, almost as great as that of BH, one might be tempted to ask the question: if the sample were doped with phosphorus instead of boron, would a similar transition from H_2 to PH take place? An experimental test was undertaken in Ref. 49, using both phosphorus and arsenic-doped samples. No infrared lines associated with PH or AsH complexes were detected, though other evidence indicated ample hydrogen concentrations.

The distinction between the behaviors of the p- and n-type samples is of course just a straightforward manifestation of the difference in ease of passivation that we have just discussed in Sec. IX (Fig. 15), a difference that arises from the asymmetrical positioning of the donor and acceptor levels of hydrogen in the band gap, and that can be expressed quantitatively via our equilibrium equations. For the deep bulk (electrically neutral) regions of a system of the type consid-

ered in Appendix B, the relevant equation is Eq. (B13) for H_2. For the present we are setting all $Z_i = 1$, and with the assumed values for ν_s of Table I in Appendix B, the factor of 2 in Eq. (B13) is changed for p-type cases to $\frac{1}{2}$ and K_{PH} is replaced by

$$K_{BH} = \Omega_0 \exp(\Delta\varepsilon_{BH}/kT), \tag{28}$$

where $\Delta\varepsilon_{BH}$ is the energy required to dissociate BH into B^- and H^+. In both cases

$$K_2 = \tfrac{3}{2}\Omega_0 \exp(\Delta\varepsilon_2/kT), \tag{29}$$

with $\Delta\varepsilon_2$ the dissociation energy for $H_2 \to H^+ + H^-$.

In terms of the total hydrogen concentration n_H, which with neglect of the small portion in monatomic form is simply

$$n_H = 2n_2 + (n_{PH} \text{ or } n_{BH}), \tag{30}$$

we can write the equilibrium condition Eq. (B13), or its appropriate modification in the form

$$n_H^3(1-f) = Af^2/[(n_I/n_H) - f]^4, \tag{31}$$

where f ($=f_{PH}$ or f_{BH}) is the fraction n_{BH}/n_H or n_{BH}/n_H of the total hydrogen bound in complexes with donors or acceptors, n_I ($=n_P$ or n_B) is the original concentration of the latter impurities, and A is either

$$A_n = (4K_2 n_i^2/K_{PH}^2)\exp[2(\langle\varepsilon\rangle - \varepsilon_m)/kT] \tag{32}$$

for n type or

$$A_p = (K_2 n_i^2/K_{BH}^2)\exp[2(\varepsilon_m - \langle\varepsilon\rangle)/kT] \tag{33}$$

for p type. If the binding energies $\Delta\varepsilon_2$ and $\Delta\varepsilon_{BH}$ or $\Delta\varepsilon_{PH}$ are known or assumed, we can calculate A_n or A_p as a function of temperature T, and then solve Eq. (31) for $f(T)$. Figure 16(a) shows a comparison of the results obtained with the values $n_H = 1.5\times10^{16}\,\text{cm}^{-3}$ and n_I ($=n_B$) $= 1\times10^{17}$ cm^{-3}, appropriate to the experiment of Ref. 50 with those that would be predicted for an n-type experiment with the same n_H and n_I (now equal to n_P). The curves are of course only intended as qualitative indicators of the expected behavior, since there are appreciable uncertainties in the binding-energy inputs, which we have selected somewhat arbitrarily (see Appendix B). $\Delta\varepsilon_{BH}$ and $\Delta\varepsilon_{PH}$ are uncertain by at least several hundredths of an electron volt; $\Delta\varepsilon_2$ is at present much more uncertain, but it cancels out of the ratio A_n/A_p. (A detailed analysis of experimental data like those of Ref. 50 might give a fair estimate, but would require a careful analysis of relaxation times and quench rates.)

The important conclusion from Fig. 16(a) is that while for n_H and n_I values similar to those used here the thermodynamically most stable state becomes that with nearly all the hydrogen on the shallow dopant at sufficiently low temperatures, whether the dopants be donors or acceptors, the temperature required in the donor case is so low that the equilibrium state cannot be reached or even approached in feasible experimental times, whereas in the acceptor case much higher temperatures and much shorter equilibration times apply. The difference between the two cases comes

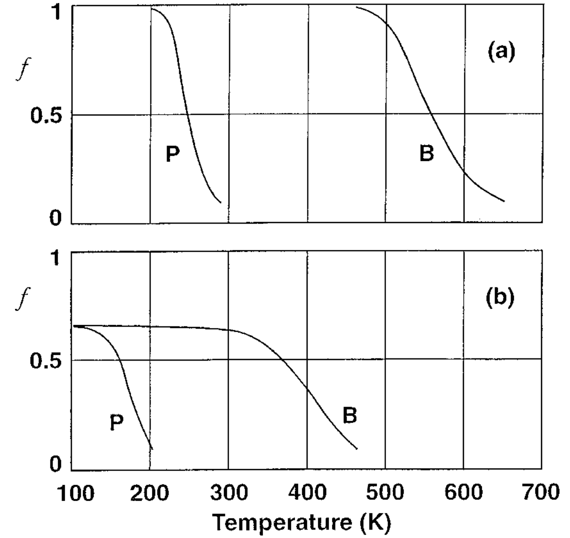

FIG. 16. Sample calculations of the degree to which hydrogen with a fixed total concentration $n_{tot} = 1.5\times10^{16}$ atoms/cm^3, in silicon, will segregate into BH complexes in boron-doped material, or into PH complexes in phosphorus-doped materials, when equilibrated at any temperature T. The vertical scale is the segregated fraction f of the total hydrogen. In (a) the B or P dopant concentration has been taken to be $1\times10^{17}\,\text{cm}^{-3}$; in (b) it has been taken as $1\times10^{16}\,\text{cm}^{-3}$. In the temperature range shown it is assumed that the only other form of hydrogen with appreciable concentration is a H_2 species with binding energy (relative to $H^+ + H^-$) of 1.80 eV.

from the different activation energies of the quantities A_n and A_p, which measure how rapidly they become small at low temperatures: the factors n_i^2 and K_{max} are the same for both cases, so cancel out of the comparison. As is discussed in Appendix B, K_{BH} is probably modestly greater than K_{PH}, the difference contributing an amount of the order of 0.1 eV to the excess of the activation energy of A_p over that of A_n; the main difference between the two cases comes rather from the factor $\exp[2(\langle\varepsilon\rangle - \varepsilon_m)/kT]$ in A_n and the inverse factor in A_p, which with our estimation of the parameters gives a contribution of about 0.65 eV to the excess activation energy of A_p over A_n. In physical terms the latter difference simply amounts to saying that, because of the asymmetrical positioning of the hydrogen donor and acceptor levels in the band gap, it is far less costly energetically to make $2H^+$ out of an H_2 in the presence of a concentration n of holes than to make $2H^-$ in the presence of the same concentration n of electrons.

The behavior shown in Fig. 16(a) persists qualitatively over quite a range in the choice of parameters. In Fig. 16(b) we show one further example, which differs from that of Fig. 16(a) in that the chemical doping n_I is slightly below the hydrogen concentration, so that the fraction f of the hydrogen complexed with dopants cannot rise to unity, and the shift of the Fermi level due to the passivation can become large.

XII. BINDING ENERGY OF H_2

As mentioned above, the (presumably diatomic) H_2 species[38] often constitutes most of the hydrogen in well-

hydrogenated n-type silicon, and its diffusional migration has been measured.[55] First-principles theoretical studies[14,56] have favored interpreting H_2 as a molecularly bound pair centered at a tetrahedral interstitial site.[57]

We shall focus on two properties of H_2, first on its binding energy $\Delta\varepsilon_2$ relative to dissociation into $H^+ + H^-$, and then, in Sec. XIII to follow, on its lifetime τ_2 with respect to this or into $2H^-$ with electron absorption. While it would be possible, and desirable, to measure both of these directly with suitably designed experiments, we shall argue that data already published provide fairly convincing evidence that $\Delta\varepsilon_2$ is large, perhaps of the order of 1.7–1.8 eV, and that in the lower part of the range of published diffusion measurements on H_2, i.e., 125–150 °C, τ_2 is probably many times larger than the duration ($\frac{1}{2}$ h) of the experiments. One can find evidence for the plausibility of both these statements in the large body of available data [Ref. 1 (Secs. III.3 and III.4 and references cited therein)] on the secondary-ion mass spectroscopy (SIMS) distributions of total hydrogen in plasma-hydrogenated n-type silicon, combined with measurements of degree of donor passivation in the same or similar specimens. In the few cases where one can plausibly expect H_2 formation and donor passivation to have been in thermodynamic equilibrium, one can use the equations of Appendix B to get a value for $\Delta\varepsilon_2$ in terms of the presumed known binding energy of hydrogen to the donor; if equilibrium seems not to have been reached, it may sometimes be plausible to assume that the observed H_2 concentration is less than that which would be in equilibrium with the observed donor passivation, so that one can extract a lower limit for $\Delta\varepsilon_2$. However, most of our attempts to analyze available data in this way, though they seem to favor the conclusions mentioned above, have been beset by uncertainties regarding equilibration, sketchiness of data on passivation, the physics of H_2 formation and dissociation, and the effect of highly inhomogeneous hydrogen densities in situations far from local equilibrium, especially the accumulation of hydrogen-rich "platelets" just beneath the surface,[58] so we shall omit a detailed discussion of these less satisfactory efforts, and focus on the analysis of the one experiment that seems more certain.

The experiment just mentioned[1] was performed on two samples of arsenic-doped epitaxial layers ($n_{As} = 3\times10^{18}$ and $0.5\times10^{18}\,\mathrm{cm}^{-3}$, respectively), each 0.9 μm thick, on substrates doped with $2\times10^{18}\,\mathrm{cm}^{-3}$ antimony. Each was deuterated for 1 h at 300 °C by the remote plasma method.[28] Subsequent SIMS analysis yielded the deuterium density distributions shown in Fig. 16. The upper trace is particularly striking: the concentration curve in each material is practically horizontal, but the levels are different for the epilayer and the substrate, with a transition region no wider than the depth range in which the concentrations are mixed (as revealed by SIMS traces for arsenic and antimony). The horizontal regions manifest the fact that, both for H_2 and for the rapidly interchanging species H^- and donor-hydrogen complexes, the diffusion coefficients at 300 °C are high enough to make the diffusion distance in an hour much greater than the depth range shown. This same fact implies that there cannot be any appreciable discontinuity in the concentration

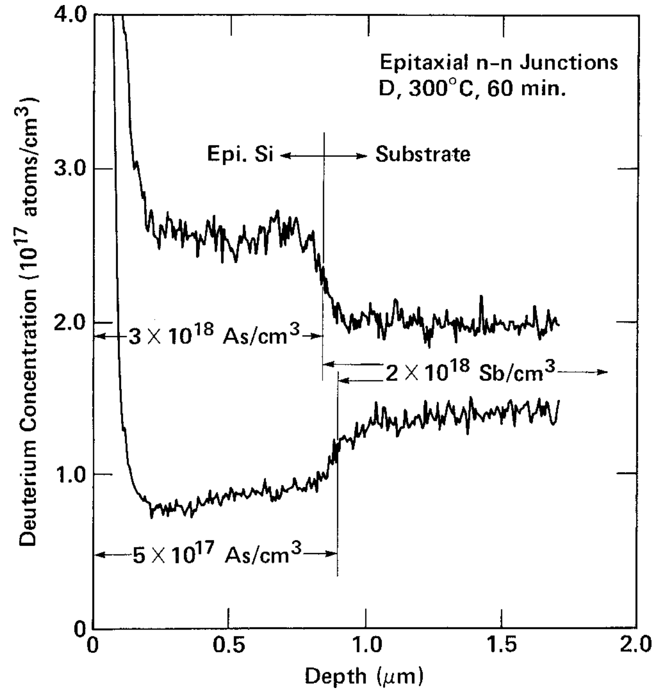

FIG. 17. Deuteration density distributions in two composite silicon samples quenched to room temperature after a 60-min deuteration at 300 °C by the remote plasma method. Both samples consisted of an arsenic-doped epilayer on an antimony-doped substrate. The thickness and doping levels of the various layers were as shown. All sample surfaces were prepared for deuteration by removing the oxide with a dilute HF etch, rinsing with distilled water, and blowing dry with flowing nitrogen.

of H_2 across the boundary: the observed discontinuity must be attributed to the concentrations of donor-hydrogen complexes, as these are the only hydrogen-containing species that could be present in significantly different concentrations on the two sides of the boundary.[59] The fact that the concentration in the epilayer is higher than that in the substrate thus means that he AsH concentration in the former exceeds the SbH concentration in the latter, and this is to be expected because of the 3:2 ratio of the respective donor concentrations, provided the difference of the binding energies $\Delta\varepsilon_{\mathrm{AsH}}$ and $\Delta\varepsilon_{\mathrm{SbH}}$ is no more than a small fraction of kT. The latter seems indeed to accord with the measurements of Bergman and co-workers.[60] In the lower trace of Fig. 17, the deuterium level is lower in the epilayer than in the substrate, as expected for the lower donor concentration in the former. However, the levels do not become quite horizontal in the interiors of the two layers, presumably because the plasma-product environment did not remain constant during the deuteration. For our analysis we have ignored this flaw, and used as inputs the ordinates of the four points where straight lines drawn through the straight portions of the epilayer and substrate SIMS plots for the two samples intersect the vertical one at the depth of the center of the junction.

If we assume that the AsH and SbH species are everywhere equilibrated with H_2, we can use Eqs. (31) and (32) to determine the difference $\Delta\varepsilon_{\mathrm{AsH}} - \Delta\varepsilon_{\mathrm{SbH}}$ and the difference $\Delta\varepsilon_2 - 2\Delta\varepsilon_{\mathrm{AsH}}$ using as inputs the four intercepts

n_H(epi,1),n_H(sub,1),n_H(epi,2),n_H(sub,2) defined in the preceding paragraph, 1 referring to the upper SIMS traces, 2 to the lower. We have four equations of the same type as Eq. (31), one for each combination of "1" or "2" with "epi" or "sub," and six unknowns namely, A_{sub},A_{epi}, and the four f's (f_{epi}, etc.). However, two of the f's, say $f_{sub,1}$ and $f_{sub,2}$, can be eliminated by the requirement that $2n_2=(1-f)n_H$ must be the same on each side of the junction, for each of the two samples:

$$(1-f_{epi,1})n_H(\text{epi},1)=(1-f_{sub,1})n_H(\text{sub},1), \quad (34)$$

$$(1-f_{epi,2})n_H(\text{epi},2)=(1-f_{sub,2})n_H(\text{sub},2), \quad (35)$$

Thus, there remain four unknowns, which can be determined from the four equations. With the input n_H's from Fig. 17, numerical solution yields

$$A_{As}=1.015\times10^{57}\,\text{cm}^{-9}, \quad (36)$$

$$A_{Sb}=0.987\times10^{57}\,\text{cm}^{-9}, \quad (37)$$

$$f_{epi,1}=0.403, \quad (38)$$

$$f_{epi,2}=0.025. \quad (39)$$

As one can see from Eq. (32), the ratio

$$A_{As}/A_{Sb}=(K_{SbH}/K_{AsH})^2=\exp[2(\Delta\varepsilon_{SbH}-\Delta\varepsilon_{AsH})/kT] \quad (40)$$

from which one gets a quite negligible difference in the two binding energies, less than 1 meV, which is far below the probable error of the measurements, and quite consistent with the earlier finding.[60]

To extract $\Delta\varepsilon_2$ from either A_{As} or A_{Sb}, we need to assume values for all the other parameters entering into the definition Eq. (32). The value $n_i(300\,°\text{C})=2.35\times10^{15}\,\text{cm}^{-3}$ is well known; for $\langle\varepsilon\rangle-\varepsilon_m$ the best we can do is to ignore its possible change with temperature and use the value 0.16 eV derived from the room-temperature $\varepsilon_A-\varepsilon_m\approx-0.07\,\text{eV}$ and $\varepsilon_D-\varepsilon_m\approx0.39\,\text{eV}$. The major uncertainty in the use of Eq. (32) comes from K_{AsH} (or K_{SbH}), that is, from the uncertainty in our knowledge of the binding energy $\Delta\varepsilon_{AsH}$ of the AsH complex. The only relevant information on this quantity seems to come from the work of Bergman and co-workers,[60] who measured by infrared spectroscopy the loss of donor hydrogen complexes from a 0.2-μm-thick donor-implanted layer, due to a series of anneals at successively higher temperatures. They found the loss to occur in the same temperature range when the donor was arsenic as when it was antimony, but to occur about 32° lower when it was phosphorus. While they quoted "binding energies" for the three complexes (1.32 eV for P-H, 1.43 eV for AsH and SbH), these do not have at all the same physical meaning as our $\Delta\varepsilon_{PH}$, etc. Rather, they are Arrhenius slopes for the observed disappearance rates, and they certainly involve the temperature dependence of the diffusion coefficient of H^-, and possibly other factors as well, depending on the precise mechanism by which the monatomic hydrogen moves out of the implanted region. (It would be incorrect to interpret their words[60] "if we assume that the donor-H complexes dissociated irreversibly..." as meaning that when a particular complex dissociates, the freed hydrogen moves out of the implanted region without ever recombining with another donor. At densities of unpassivated donors of the order of $10^{19}\,\text{cm}^{-3}$, the mean diffusion distance of an H^- before trapping by a donor is, thanks to the large Coulomb capture radius, only a few nanometers.) Their measurements do, however, establish that the binding energy $\Delta\varepsilon$ is very nearly the same for AsH and SbH, and appreciably larger for these than for PH.

It might seem plausible to equate the excess 0.11 eV of the activation energy for AsH and SbH over that for PH to $\Delta\varepsilon_{AsH}-\Delta\varepsilon_{PH}$, since diffusion coefficients, etc., should be the same in all cases. This would indeed be correct if the disappearance rate had the form $F\exp[-(\Delta\varepsilon+Q)/kT]$ with Q independent of the donor and F equal to their assumed prefactor $10^{13}\,\text{s}^{-1}$. However, the actual prefactor may well be very different from this assumed value, and the "activation energies" determined from a rough fit to the annealing rates will depend significantly on the prefactor assumed. So although we shall, for want of a better value, assume $\Delta\varepsilon_{AsH}=\Delta\varepsilon_{PH}+0.11\,\text{eV}=0.84\,\text{eV}$ in our evaluation of $\Delta\varepsilon_2$, by equating Eqs. (32)–(36) and solving for $K_2=\Omega_0\exp(\Delta\varepsilon_2/kT)$, we do so with the realization that the possible error in $\Delta\varepsilon_{AsH}$ is compounded by that in $2\Delta\varepsilon_{PH}$ and a rather larger uncertainty in $2(\Delta\varepsilon_{AsH}-\Delta\varepsilon_{PH})$. These approximations yield

$$\Delta\varepsilon_2\simeq1.75\,\text{eV}. \quad (41)$$

While the uncertainties in the inputs, discussed above, could make this figure uncertain by as much as 0.1 eV or even more, Eq. (41) is surprisingly large compared to what one might have expected from first-principles theoretical calculations. Addition of our $\varepsilon_D-\varepsilon_A=0.45\,\text{eV}$ to Eq. (41) gives an "empirical" value of 2.20 eV for the energy to dissociate H_2 into $2H^0$, while density-functional calculations[61] using the local-density approximation give only 1.74 eV. Both the experimental and theoretical approaches need to be examined more carefully. We can mention here just two further pieces of information that may be indicative. One is that the fit of the upper right-hand curve of Fig. 16 to the experimental points of Ref. 50 is fairly good near the high temperature end (although we did not attempt to optimize this fit), and since in this region the departure from equilibrium was probably quite small, this means that the value of $\Delta\varepsilon_2$ we assumed in calculating the curve (1.80 eV) must have been nearly correct. The other item is that a recent density-functional study of silicon self-interstitials[62] found quite sizable changes in their formation energy (≈0.5 eV) when the local approximation to the exchange-correlation functional was replaced by the generalized gradient approximation. So it may well be that the local-density approximation, though it works well in many cases, is less accurate for $\Delta\varepsilon_2$.

XIII. KINETICS OF FORMATION, DISSOCIATION, AND MIGRATION OF H_2

In our measurements of the diffusion coefficient of H_2,[39] we had no way to be sure whether the migrating H_2 remained

as an associated pair of hydrogen atoms at all times, or whether it dissolved from time to time into separated monatomic species, which could migrate rapidly for a short time and then recombine into H_2 again. We can now show with fair certainty that the latter process must have been negligible over the temperature range of the experiments ($T \leqslant 200\,°C$); the molecules must have migrated as units, though perhaps passing through distorted configurations during their hops.

The core of our argument is to use the rough value Eq. (41) of the binding energy of H_2 to set a rough upper limit on its dissociation rate at any temperature T in the range of interest. This has to be done carefully, as it may happen that the dissociation rate depends on the environment, especially the electron concentration. In the absence of electronic carriers, an isolated H_2 can dissociate into H^+ and H^- a few atom spacings apart, which can then fluctuate against their mutual Coulomb attraction, and occasionally to a large distance. The lifetime $\tau_2^{(i)}$ with respect to such an "isolated" dissociation should be given with fair accuracy by the familiar expression (Ref. 63 and Sec. II.2 of Ref. 1)

$$1/\tau_2^{(i)} = 4\pi(D_+ + D_-)R_C \exp[-\Delta\varepsilon_2/kT]/\Omega_0, \quad (42)$$

where R_C is the Coulomb capture radius $e^2/\kappa kT$. However, numerical evaluation of this expression with the 1.75 eV for $\Delta\varepsilon_2$ of Eq. (41) yields dissociation times too long to be believable for the conditions of the type of experiments we have been discussing, for example, from a few times 10^{13} s at 130 °C to a few times 10^8 s at 200 °C and around 10^4 s at 300 °C. A more serious limitation of Eq. (42) is that its use to compute, by the principle of detailed balance, the rate of formation of H_2 by the inverse process $H^+ + H^- \rightarrow H_2$ gives values far lower than the observed rate of formation in experiments like those of Ref. 55 at 130 °C. This failure does not depend on the value of $\Delta\varepsilon_2$, being due simply to the rarity of H^+ in strongly n-doped material. Clearly a different path for formation and dissociation must be dominant.

What sort of alternative mechanisms could exist? An obvious possibility is that after H_2 has dissociated part way into H^+ and an H^- just a few atom spacings apart, the H^+ might absorb two electrons to become an H^-, subject to repulsion from its former H^- mate; this only accelerates the dissociation. But unless the two electrons were absorbed essentially simultaneously, the system would have to exist temporarily as $H^+ + H^0$, and unless the Fermi energy were above the hydrogen-donor level, as it is not in most of the experiments we have been discussing, this configuration would be expected to have an even higher free energy than H^- plus an H^+ at infinity. This difficulty might conceivably be avoided if the first charge change took place at an interhydrogen separation r small enough to render the behavior of the "H^+" rather different from that of an isolated H^+ in a uniform electrostatic potential equal to $-e/\kappa r$. Alternatively, one might speculate that the dissociation and formation processes are dominated by catalytic effects, for example, involving interaction with shallow donors.

Consider first the dissociation of an H_2 interacting only with the silicon lattice and the conduction electrons. For each

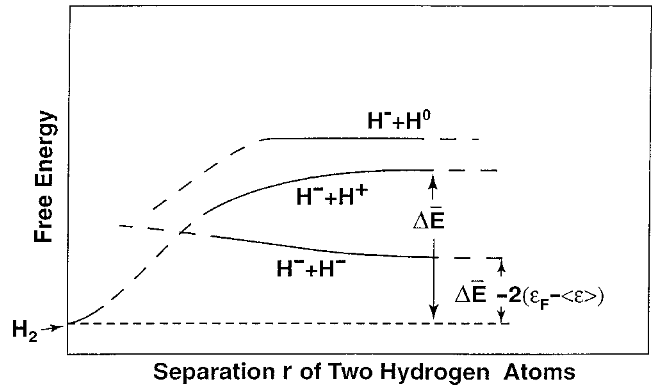

FIG. 18. Hypothetical variation of the free energy of two monatomic hydrogen atoms with their separation r, when they are coupled to a sea of conduction electrons. (The "free energy" plotted is actually the local minimum of the free energy that occurs when both atoms are at lattice sites that are locally free-energy minima near the given r; the barrier free energies that must be surmounted for each successive hop are not shown.)

metastable configuration of the two dissociating hydrogens the system hydrogens plus electrons will have a certain free energy, whose dependence on the separation of the hydrogens will look something like Fig. 18 (quite possibly dependent on direction, at small r). The effective free-energy barrier that the system must surmount in order to escape to large separation will depend not only on the curves shown, but also (in a complicated way) on the hopping frequencies between adjacent sites and on the rates of emission or absorption of electrons to change the charge state of a hydrogen. However, this barrier can never be less than the asymptotic height of the bottom curve above the ground-state free energy of H_2. So we may expect the dissociation rate to contain a barrier-height factor at least as small as $\exp\{[\Delta\varepsilon_2 - 2(\varepsilon_F - \langle\varepsilon\rangle)]/kT\}$. The prefactor, like that in Eq. (42), will contain a diffusion coefficient compounded out of D^+, D^-, and D^0, the reciprocal of the unit cell volume Ω_0, and an effective radius of the order of the r at which the transition to the $H^- + H^-$ curve becomes effective (less than R_C if the barrier lowering below $\Delta\varepsilon_2$ is appreciable). So it is not unreasonable to assume that for the present case of interactions only with electrons

$$1/\tau_2 \leqslant [1/\tau_2^{(i)}]\exp[2(\varepsilon_F - \langle\varepsilon\rangle)/kT]. \quad (43)$$

Could catalytic processes lead to more rapid dissociation? The simplest competing process would be for a mobile H_2 to encounter a P^+ and undergo a reaction

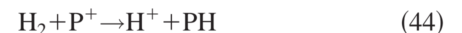

$$H_2 + P^+ \rightarrow H^+ + PH \quad (44)$$

followed by separation of the products on the right and subsequently by readjustment of equilibria. We have examined possible details of such a process[64] and have not found a plausible scenario that with an acceptor concentration of $3\times 10^{18}\,cm^{-3}$ could give a perceptible dissociation rate at 200 °C, or an easily measurable one at 300 °C. By contrast, the limit in Eq. (43) for the purely electron-assisted

process is for 2×10^{18} donors/cm^3 and 300 °C, and with the doubtless too high extrapolation $D^-(300\,^\circ\mathrm{C})\approx10^{-6}$ cm^2/s,

$$1/\tau_2\leqslant 0.05\ \mathrm{s}^{-1}, \qquad (45)$$

that is, merely requires a dissociation time longer than tens of seconds.

Now we are ready to draw useful conclusions about the order of magnitude of τ_2 for the conditions under which the measurements of D_2 were carried out,[55] namely, temperatures of 200 °C and below, and phosphorus concentrations of 1×10^{17} and 8×10^{17} cm^{-3}. Neglecting the catalytic process, we can use Eq. (43) to get a (doubtlessly extreme) upper limit on $1/\tau_2$, which comes out to be

$$1/\tau_2\leqslant 5\times10^{-7}\ \mathrm{s}^{-1} \qquad (46)$$

for the worst case among the diffusion profiles plotted in Fig. 1 of the earlier work[39] (200 °C, $n_\mathrm{P}=1\times10^{17}$ cm^{-3}). Thus in this case, and *a fortiori* for all the other diffusion profiles plotted in this figure, there should not have been any detectable contribution of dissociation and recombination to the observed migration in a $\frac{1}{2}$-h anneal. Except for the redistribution of the small amount of hydrogen present as H^- or PH, all the observed migration must almost certainly have been due to motion of H_2 "molecules" as whole entities, without dissociation, though doubtless with momentary distortion. This conclusion of course rests on the assumption that the binding energy of H_2 relative to H^+ and H^- is of the order of the 1.75 eV of Eq. (43). But for the conclusion to fail, a binding energy lower by at least several tenths of an eV would be needed.

XIV. CONCLUSIONS

In the first part of this paper, we have addressed the experimental problem of controllable creation of monatomic hydrogen (or deuterium) followed by measurement of the equilibrium and dynamic properties of the monatomic species in their different charge states. The preparation of monatomic hydrogen was achieved by first hydrogenating the near-surface region of a phosphorus-doped silicon wafer, then evaporating a metal electrode onto the hydrogenated surface and then drawing into the Schottky barrier thus formed a brief pulse of minority holes optically generated on the opposite side of the wafer. By holding the Schottky barrier under reverse bias during and after the hole pulse, the sudden change in capacitance produced by the pulse and the gradual relaxation to a new value in the course of time after the pulse, it became evident that essentially all of the monatomic hydrogen became positively charged by autoionization, and then drifted rapidly out the front surface without being captured by phosphorus or otherwise trapped.

To measure the donor energy of hydrogen it was necessary to study the transition between the neutral and positive charge states. But since the acceptor level turns out to lie well below the donor level, the concentration of neutrals is always very low compared with the other species if charge-exchange equilibrium is allowed to occur. We found that an appreciable concentration of neutrals could, however, be obtained by quenching our samples rapidly to low temperature at zero bias immediately after the hole pulse. It was then possible to study the spontaneous ionization of the neutral species in the diode by DLTS. After correction for the lowering of ionization energy by the electric field in the diode, our result is in reasonable agreement with the position reported in the literature for the donor level of the so-called $E3'$ center in proton-bombarded silicon, namely, about 0.16 eV below the conduction band. This confirms that the $E3'$ center is indeed a hydrogen atom in its equilibrium position surrounded by undamaged crystal. From this ε_D and measurements of the rates of the changes $H^+\rightarrow H^-$ on flooding the diode with electrons and $H^-\rightarrow H^+$ on imposing reverse bias, we have been able to determine the position of the acceptor level ε_A by using the principle of detailed balance and the assumption, reasonably confirmed by first-principles calculations of the dependence of electronic energies on lattice position for a hydrogen atom, that the migration associated with the charge changes is not appreciably delayed by residence at an intermediate metastable position. The ε_A obtained was slightly below midgap, or about 0.62 eV below the conduction-band edge, at room temperature.

The rates of the phonon-mediated reactions $H^0\rightarrow H^+ + e^-$ and $H^-\rightarrow H^0+e^-$ have very different activation energies. For the former, the above-mentioned 0.16-eV activation energy gives a transition time at room temperature (extrapolated from the low-temperature measurements) in the subnanosecond range, whereas the latter transition, with an activation energy of 0.84 eV, is of the order of a second at room temperature. The fact that the activation energy is several tenths of an electron volt greater than the energy difference between initial and final states indicates that the electron loss occurs when the atom is at an intermediate lattice site where the energy of the neutral atom is significantly higher than the energy in the final bond-centered position.

The mobilities, or equivalently the diffusion coefficients D_+ of positively charged hydrogen and deuterium have been inferred from the rate of sweep-out of the freshly prepared species in reverse-biased diodes. Over the range 300–320 K the data are well fitted by $D_+(^1H^+)=1.45\times10^{-3}\exp(-0.50\,\mathrm{eV}/kT)$ and $D_+(^2H^+)=1.44\times10^{-3}\exp(-0.51\,\mathrm{eV}/kT)$ cm^2/s. Our values for $D_+(^1H^+)$ fall very close to the extrapolated Arrhenius line obtained by van Wieringen and Warmholtz[2] at temperatures above 1000 K, and also with the extrapolation of the diffusion coefficient that can be inferred from the local hopping rates measured by Gorelkinskii and Nevinnyi[24] at temperatures below 145 K. One can conclude that proton tunneling does not play a role in the latter measurements. The room-temperature ratio of the D_+ values is about 1.9, and seems to be caused as much by the isotopic difference in zero point energies as by that in thermal velocities. A diffusion coefficient of H^- has also been measured, though more crudely, via the rate of recombination of ^2H with P^+ when the diode is held at zero bias. At 300 K, $D_-(^2H^-)$ is about 3×10^{-12} cm^2/s, close to the value of $D_+(^2H^+)$, but its activation energy seems to be higher, though not more than 0.70 eV.

The later sections of this paper discuss a number of examples that show how the previously described properties of monatomic hydrogen in silicon, notably the "negative-U" positioning of the donor and acceptor levels, enable natural explanations to be given for a number of previously known but unexplained properties of hydrogenated silicon. A simple example is the well-known fact that it requires a much more intense hydrogenation to produce a given degree of passivation in phosphorus-doped silicon than in material boron-doped to the same concentration. We show that this fact is due mainly to the extremely asymmetric positioning of the hydrogen donor and acceptor levels in the gap, and only slightly to the small difference between the binding energy of P^+ to H^- and that of B^- to H^+.

A similar difference arises in regard to the dissociation of donor-hydrogen and acceptor-hydrogen complexes by minority carriers. While the dissociation of PH complexes by minority holes has been generally accepted in the literature, and has served as a very reliable source of monatomic hydrogen in the experiments described earlier in this paper, conflicting conclusions have been drawn in the literature regarding the analogous dissociation of BH complexes by minority electrons. We have attempted to produce such dissociations at room temperature using the same type of experimental arrangement as that used for our PH dissociations, and have not been able to measure an observable effect: the cross section for dissociation of BH by e^- at 320 K must be less than a few percent of that for dissociation of PH by h^+ at 270 K, the temperature at which thermal dissociation of PH is about the same as that of BH at 300 K. We show theoretically that there should be a great difference between the two cases because at temperatures near and above room temperature the H^0 formed in the early stages of dissociation will quickly autoionize and be drawn back to the B^- in the BH case, whereas it will be repelled from the P^+ in the PH case. We have considered the possible effects of an extremely high diffusion coefficient for the H^0 species on the kinetics of the dissociation process, and concluded that efficient BH dissociation due to this property is not likely.

We show that useful information can be obtained by studying the equilibrium of monatomic species with the diatomic species now generally believed to be the neutral, spinless, fairly mobile species frequently abundant in hydrogenated n-type silicon, and sometimes in p type. We have now used the presently available information on the donor and acceptor levels of monatomic hydrogen to analyze data previously published by us on the distribution of total deuterium concentration in and beneath n-on-n epitaxial layers with different arsenic concentrations on antimony-doped substrates. By assuming all species to be equilibrated locally at the end of hydrogenation, we found that a fit to the observed discontinuity across the interface in the local concentration of total hydrogen could be fitted only by assuming a rather large value, near 1.75 eV, for the binding energy of $^2H_2$ with respect to dissociation into $^2H^+$ and $^2H^-$. This binding energy is roughly confirmed by the approximate agreement, in the range above 400 K between the calculated equilibrium concentration ratios of H_2 and BH and those observed in the measurements of Ref. 50 when the binding energy was arbitrarily assumed to be 1.8 eV. A more accurate fit over a wider temperature range can be made when data allowing time to achieve equilibrium at lower temperatures are available.

The high binding energy now found for the H_2 species provides strong support for the view that its migration at temperatures of 200 °C and below is by diffusion of undissociated units, rather than by dissociation temporarily into monatomic hydrogen followed by recombination later. This is consistent with the fairly accurate Fickian behavior observed in Ref. 39. However, it does not rule out the possible occurrence, during diffusion, of configurations of the migrating pair in which the two hydrogens have temporarily separated from each other by one or two atom spacings.

The strongly asymmetric positions of the donor and acceptor levels of hydrogen in the gap provide a natural explanation of the observed fact that hydrogen, introduced into silicon at high temperatures, easily associates itself on cooling with boron atoms in boron-doped silicon, whereas efforts to observe a similar association with phosphorus atoms in phosphorus-doped silicon have failed. Quantitative calculations of the temperature dependence of the equilibrium distribution of hydrogen between the H_2 species and the BH species or between H_2 and PH show that although the transferal occurs in both cases, it becomes appreciable in the phosphorus case only at temperatures much lower than those for the boron case. Like the difference in ease of passivation for comparably doped n- and p-type silicon, the difference is due more to the asymmetric positioning of the donor and acceptor levels than to the small difference in the binding energies of the dopant-hydrogen complexes.

APPENDIX A: CAPACITANCE TRANSIENT AS A CHARGE MOMENT

The capacitance transients studied in the present paper arise from the initial generation of new charged species (P^+ and H^+), the ensuing motion of the H^+, its possible conversion to H^- and possible H^--P^+ recombination. At all stages the total number of these new entities in the depletion region of the diode is a small fraction of the number of ionized donors initially present, and this fact makes it possible to use a very simple relation between the measured capacitance change $\Delta C(t)$ and the spatial distribution of the newly created charge density $\Delta\rho(x,t)$. We use the standard depletion-layer approximation in which a depletion layer with a density $\rho(x)$ of ionic charge ends at depth W_D, beyond which the sum of electronic and ionic charge densities is assumed to be everywhere zero. For a diode with a metal electrode at $x=0$ these assumptions give for the applied voltage V_R in a reverse-bias configuration

$$V_R=\frac{4\pi}{\kappa}\int_0^{W_D}x\rho(x)dx-V_B+[\varepsilon_C(W_D)-\varepsilon_F(W_D)]/e, \tag{A1}$$

where κ is the dielectric constant, eV_B is the barrier height $\varepsilon_C-\varepsilon_F$ at the metal-semiconductor interface, $\varepsilon_C(x)$ is the energy of the conduction-band edge, and $\varepsilon_F(x)$ the Fermi

level, or for $V_R \neq 0$ the quasi-Fermi-level of the electrons. The integral represents the variation of electrostatic potential across the depletion layer, and the two last terms allow for the different positions of ε_F relative to ε_C at $x=0$ and $x=W_D$, respectively. When a small change $\delta\rho(x)$ is made in the charge distribution, while holding V_R constant and assuming that V_B does not change, we have

$$0=\frac{4\pi}{\kappa}\left(\int_0^{W_D} x\,\delta\rho(x)dx+W_D\rho(W_D)\,\delta W_D\right)-\frac{kT}{e}\,\delta[\ln\rho(W_D)]. \tag{A2}$$

We have used the assumption

$$\rho(W_D)\propto \exp\left[\frac{\varepsilon_F-\varepsilon_C}{kT}\right],$$

valid if the carriers are nondegenerate, to evaluate the variation of the last term in Eq. (A1). However, if $\rho(x)$ and $\delta\rho(x)$ each vary gradually on a scale of order W_D, it is easily seen that, upon expansion, the two parts of the last term of Eq. (A2), proportional, respectively, to $\delta\rho(W_D)$ and to $\delta W_D(\partial\rho/\partial x)_{W_D}$, are in general smaller than the corresponding parts of the first term by factors of the order of the ratio of kT to the band bending [i.e., charge e times the first term of Eq. (A1)], which is a fraction of a percent in our experiments. Thus, it is a good approximation to neglect this term and set the term in large parentheses in Eq. (A2) equal to zero. Since the differential capacitance C of the depletion layer is given by[65]

$$C=4\pi\kappa A/W_D,$$

where A is the diode area, we then have

$$-\frac{\delta W_D}{x_D}=\frac{\delta C}{C}=\frac{\int_0^{W_D}x\,\delta\rho(x)dx}{W_D^2\rho(W_D)}=\frac{C^2\int_0^{W_D}x\,\delta\rho(x)dx}{(4\pi\kappa A)^2\rho(W_D)}. \tag{A3}$$

This expression reveals that the change in capacitance with time is proportional to the first spatial moment of the change in charge density within the depletion layer. Equation (A3) is generally applicable to the analysis of conventional DLTS data as well as to the more complex cases analyzed in the present study.

APPENDIX B: CONCENTRATION RATIOS IN THERMODYNAMIC EQUILIBRIUM

Many of the conclusions of this paper, especially those of Secs. VIII–XIII, result from the relations that must exist between the concentrations of various hydrogen species or complexes whenever local thermodynamic equilibrium has been established. As derivation of each such relation where it is used would either entail repetition or else require clumsy cross-referencing, we shall derive most of the needed relations once and for all in this appendix.

For practically all our purposes it will suffice to restrict consideration to systems containing only the following species (concentration variable in parentheses):

(1) electrons (n_e, hole concentration negligible);

(2) monatomic hydrogen (n_+, n_0, or n_-);

(3) one kind of shallow-donor atoms and their complexes with hydrogen (n_{P^+},n_{PH}, or the corresponding species with As, etc., substituted for P throughout);

(4) one kind of diatomic hydrogen complex (n_2, if we take this species to be the species whose diffusion was measured in Ref. 55).

If such a system is allowed to alter the concentrations of the various species listed by exchanging charges or atoms among these species, its possible thermodynamic equilibrium states at any temperature T and state of strain can have only three further degrees of freedom, which we might for example take to be the chemical potentials of the three independent constituents: electrons, shallow donors, and hydrogen. Actually we are free to choose any three intensive variables that are independent functions of these, and our choice for the formulas to be tabulated below will be a set that is easily known or measurable in practical cases, namely, n_P, n_{P^+}, and either n_e or the corresponding Fermi level height ($\varepsilon_F-\varepsilon_m$) above midgap. In the deep bulk, away from surfaces, there is a constraint of charge neutrality, which reduces the three independent variables s to two, which we shall take to be n_P and n_{P^+}.

We start by listing the equilibrium equations that suffice for the determination of all the other variables in terms of the chosen three independent ones. In the accurate form of these equations [Ref. 1 (Sec. II.1)], one must take account, for each impurity or complex species s, of the number ν_s of sites or orientations possible for this species per unit cell, and of the modification which each unit of this species makes in the vibrational partition function of the host plus impurity atoms. This latter modification is given by an effective partition function Z_s, which becomes unity as $T\to 0$, and is larger for $T>0$. (In the present work we have always used the low-temperature approximation $Z_s=1$, but for possible future applications we shall show here how the results depend on Z_s.) Table I lists the ν_s values for the currently accepted models of the various entities with which we are concerned; these include spin degeneracy when it is present. We can write down a particularly simple set of basic equations from which

TABLE I. Numbers ν_s of equivalent configurations, per unit cell (two-silicon-atom sites) for the various entities s.

Entity s	Assumed model	ν_s
H^+	Bond-center site	4
H^0	Bond-center site, either spin	8
H^-	Tetrahedral site	2
P^+	Substitutional site	2
PH	H at antibonding site of a Si neighbor of P	8
BH	H at bond-center site next to B	8
H_2	H_2 molecule at tetrahedral site[a] oriented along [100]-type direction	6

[a]Reference 57

TABLE II. Volume concentrations of the various entities, listed in the first column, in terms of the chosen independent variables n_P, n_{P^+}, and (if charge neutrality does not hold) ε_F. Hole concentration has been assumed negligible, and all vibrational partition function factors Z_s have been set equal to 1. The entries in the penultimate column immediately to the left must be multiplied to take into account the effect of the finiteness of the monatomic hydrogen concentration (to first order only). The quantity ϕ is defined as follows: $\Phi \equiv 1-(n_P-n_{P^+})\{1-2(n_i/n_{P^+})^2 \exp[2(\langle\varepsilon\rangle-\varepsilon_m)/kT]\}/(Kn_{P^+}^2)$.

Entity, Concentration	General (neutral or not)	With charge neutrality, assuming $n_\pm, n_0 \ll n_{PH}, n_2$	Correction factor	Eq. no.
e, n_e	$n_i \exp[(\varepsilon_F-\varepsilon_m)/kT]$	n_{P^+}	Φ	(B8)
H^-, n_-	$(n_P-n_{P^+})/(Kn_{P^+})$	$(n_P-n_{P^+})/(Kn_{P^+})$	1	(B9)
H^0, n_0	$\dfrac{4(n_P-n_{P^+})\exp[(\varepsilon_A-\varepsilon_F)kT]}{Kn_{P^+}}$	$\dfrac{4(n_P-n_{P^+})n_i \exp[(\varepsilon_A-\varepsilon_m)/kT]}{Kn_{P^+}^2}$	Φ^{-1}	(B10)
H^+, n_+	$\dfrac{2(n_P-n_{P^+})\exp[2(\langle\varepsilon\rangle-\varepsilon_F)kT]}{Kn_{P^+}}$	$\dfrac{2(n_P-n_{P^+})n_i^2 \exp[2(\langle\varepsilon\rangle-\varepsilon_m)/kT]}{Kn_{P^+}^3}$	Φ^{-2}	(B11)
PH, n_{PH}	$n_P-n_{P^+}$	$n_P-n_{P^+}$	1	(B12)
H_2, n_2	$\dfrac{2K_2(n_P-n_{P^+})^2\exp[2(\langle\varepsilon\rangle-\varepsilon_F)/kT]}{K^2n_{P^+}^2}$	$\dfrac{2K_2(n_P-n_{P^+})^2 n_i^2 \exp[2(\langle\varepsilon\rangle-\varepsilon_m)/kT]}{K^2n_{P^+}^4}$	Φ^{-2}	(B13)

all the equilibrium concentrations can be inferred. First,

$$n_e = n_i(T)\exp[(\varepsilon_F-\varepsilon_m)/kT], \tag{B1}$$

where $n_i(T)$ is the intrinsic concentration; the temperature dependence of the energy gap and density of states are taken into account by the empirical form of this function. However, electron-interaction effects are not allowed for, so Eq. (B1) should be used only in the nondegenerate range. Next,

$$n_+ = (\nu_+ Z_+/\nu_0 Z_0) n_0 \exp[(\varepsilon_D-\varepsilon_F)/kT], \tag{B2}$$

where ε_D is the hydrogen donor level, and

$$n_- = (\nu_- Z_-/\nu_0 Z_0) n_0 \exp[(\varepsilon_F-\varepsilon_A)/kT], \tag{B3}$$

where ε_A is the hydrogen acceptor level. Again

$$n_{PH} = (\nu_{PH} Z_{PH}/\nu_{P^+} Z_{P^+} \nu_- Z_-)\Omega_0 n_- n_{P^+} \exp(\Delta\varepsilon_{PH}/kT) \equiv K_{PH}(T) n_- n_{P^+}, \tag{B4}$$

where $\Delta\varepsilon_{PH}$ is the binding energy of P^+ and H^- into PH. And finally,

$$n_2 = (\nu_2 Z_2 \Omega_0/\nu_+ Z_+ \nu_- Z_-) n_+ n_- \exp(\Delta\varepsilon_2/kT), \tag{B5}$$

where Ω_0 is the volume of the (two-silicon-atom) unit cell and $\Delta\varepsilon_2$ is the binding energy of H^+ and H^- into H_2.

The equations expressing the various concentrations in terms of the chosen set of independent variables are given in Table II; they all follow from simple combinations of Eqs. (B1)–(B5) with the conservation laws

$$n_P = n_{P^+} + n_{PH} \tag{B6}$$

and, when electrical neutrality is imposed,

$$n_{P^+} + n_+ = n_e + n_-. \tag{B7}$$

Thus, for example we can replace the independent variable n_0, which is inconvenient because it is never directly measurable, by our chosen variables n_P and n_{P^+}, by using Eq. (B3) to get n_0 in terms of n_-, then Eqs. (B4) and (B7) to get n_- in terms of n_P and n_{P^+}. In most situations, at temperatures $\leqslant 300\,°C$, the concentrations of the monatomic hydrogen species are much smaller than those of the complexes PH and H_2, so one makes little error in neglecting the former relative to the latter whenever they occur in competition. Since this considerably simplifies some of the formulas in Table II, we have made this simplification in the fourth column of the table. However, to deal with cases where greater accuracy is needed we have given in the next column the correction factor needed to describe the first-order effect of the monatomic concentrations.

A completely analogous set of equations can be written for p-type material (say B-doped). Equations (B2), (B3), and (B5) need no modification; Eqs. (B1), (B6), and the equations of Table II [Eqs. (B8)–(B13) are found in the table] can be replaced by their "symmetrical counterparts" with, in some cases, changes in the numerical coefficients due to the use of different numbers for the degeneracies ν_i (cf. Table I). What we have called "symmetrical counterparts" are expressions related by the exchanges

$$\begin{aligned}
&\text{subscripts or superscripts:} && + \Leftrightarrow -; \\
&\text{subscripts:} && e \Leftrightarrow h, \quad D \Leftrightarrow A, \quad \mathrm{P} \Leftrightarrow \mathrm{B}; \\
&\text{every} && e \Leftrightarrow -e; \\
&\text{every} && \exp[(\ )] \Leftrightarrow \exp[-(\ )].
\end{aligned} \tag{B14}$$

The changes of numerical coefficients are needed only in middle columns of Eqs. (B10), (B11), and (B13) in Table II, where

in Eq. (B10): 4 for n type $\Leftrightarrow$ 2 for p type;

in Eqs. (B11) and (B13):

$$2 \text{ for } n \text{ type} \Leftrightarrow \tfrac{1}{2} \text{ for } p \text{ type}; \tag{B15}$$

and in the correction factor Φ where

$$2 \text{ for } n \text{ type} \Leftrightarrow \tfrac{1}{2} \text{ for } p \text{ type}. \tag{B16}$$

Finally, the K coefficient in the equations of Table II, given by Eq. (B4) for n type, becomes

$$K_{\mathrm{BH}} = [\nu_{\mathrm{BH}} Z_{\mathrm{BH}} / (\nu_{\mathrm{B^-}} Z_{\mathrm{B^-}} \nu_+ Z_+)] \Omega_0 \exp(\Delta\varepsilon_{\mathrm{BH}}/kT) \tag{B17}$$

for p type, that is, has half the numerical coefficient of K_{PH} in the low-temperature limit.

It is appropriate to say a few words here about our choice of inputs for numerical calculations using formulas like those of Table II. Besides the quantities that vary from experiment to experiment (dopant concentrations, etc.), there are several that are fixed properties of silicon or of specific impurities. One of these, $n_i(T)$, is well known, but the energy levels $\varepsilon_D, \varepsilon_A$, and the binding energy $\Delta\varepsilon_{\mathrm{PH}}$ have only recently been measured, and their values are still modestly uncertain; possible new experiments in the near future could yield more definitive values. For the present we have simply used our own best guesses, which we shall now describe. The principal information on the donor level ε_D comes from DLTS measurements[21,66] and equilibration measurements[23] on the H^0/H^+ transition at low temperatures (cf. Sec. V B). The extrapolation to zero field is still somewhat uncertain, but we now favor the value 0.16 eV for $\varepsilon_C - \varepsilon_D$ instead of the value 0.20 eV used in Ref. 27. Since the ε_A determined in Ref. 27 was dependent on ε_D, we now prefer $\varepsilon_A = \varepsilon_m - 0.064$ eV instead of the $\varepsilon_m - 0.05$ eV of the published erratum to Ref. 27.

As for $\Delta\varepsilon_{\mathrm{PH}}$, our best source of information at present comes from measurements of the rate of dissociation $1/\tau_{\mathrm{PH}}$ of the PH complex, which in the absence of external fields should be given by [Ref. 1 (Sec. II 2)]

$$\begin{aligned} 1/\tau_{\mathrm{PH}} &= 4\pi[\nu_{\mathrm{P^+}} Z_{\mathrm{P^+}} \nu_- Z_- / (\nu_{\mathrm{PH}} Z_{\mathrm{PH}})](D_- R_C/\Omega_0) \\ &\quad \times \exp(-\Delta\varepsilon_{\mathrm{PH}}/kT) \\ &= 2\pi (D_- R_C/\Omega_0) \exp(-\Delta\varepsilon_{\mathrm{PH}}/kT). \end{aligned} \tag{B18}$$

The dissociation rate of PH has been measured over the range 328–348 K from the decrease in the PH concentration upon annealing diodes under reverse bias, and noting the decrease in concentration of PH in the regions closest to the surface, where recombination of P^+ with H^- released from dissociating complexes at shallower depth should be slight.[7] However, the high field in this region (on average about 1.6×10^5 V/cm) significantly lowers the Coulomb barrier for the final escape of H^- from P^+, and thus increases the dissociation rate of PH compared with what it would be in a field-free region. For fields and temperatures of the magnitudes relevant for this experiment the departure from Eq. (B18) can be reasonably well calculated using a strong-field approximation.[67] For our present purpose we have chosen to analyze one of the better measurements of Fig. 3 of Ref. 7, namely, the measurements at early to moderate annealing times for the point at 65 °C. The observed "dissociation rate" plotted there needs to be augmented by about 20% to correct for recombination capture of H^- released from depths shallower than the limit of the observed profile; correction for the barrier lowering by the electric field gives a zero-field dissociation rate about $\frac{2}{3}$ that in the field. Inserting the thus-corrected τ_{PH} into Eq. (B18), along with $D_-(65\,^\circ\mathrm{C}) \approx 6.5 \times 10^{-11}\,\mathrm{cm^2/s}$, extrapolated from the data of Ref. 8, we obtain

$$\Delta\varepsilon_{\mathrm{PH}} = 0.71 \text{ eV} \quad (\text{for P }^2\mathrm{H}) \tag{B19}$$

This is somewhat uncertain not only because of the various adjustments of the inputs described above, but also because we have ignored the temperature-dependent Z_i's in the prefactor, which are probably necessary if the Arrhenius slope of the dissociation rate is to be adequately understood, and because, as remarked in Ref. 8, both the reported D_- and its Arrhenius slope may have been slightly too large. However, these uncertainties should not be large enough to have a major effect on the conclusions of the present paper and we shall use the value Eq. (B19) throughout.

In the few places where calculations are made for p-type material, $\Delta\varepsilon_{\mathrm{BH}}$ is used. Rough values for this can be inferred in various ways from data in the literature. An obvious source is the careful measurements made by Zundel and Weber[41] on the dissociation of BH complexes in biased diodes. These authors determined dissociation rates at various temperatures by annealing biased diodes and measuring the rate of disappearance of BH at the shallowest depths at which it could be measured, as described above for the slightly later work of Ref. 7 on PH. Again, no corrections for field-enhanced dissociation or for recapture of monatomic species released in dissociation nearer the surface were made; however, these were probably even smaller than for the data of Ref. 7. Neglecting them, and carrying out an analysis similar to that used above for PH, we get

$$\Delta\varepsilon_{\mathrm{BH}} = 0.77 \text{ eV} \quad (\text{for B }^1\mathrm{H}) \tag{B20}$$

We shall use this, though it is even more questionable than Eq. (B19), and shall ignore the possibly small isotope dependence; our interest is mainly in the qualitative differences between n-and p-type behavior. Studies of the tails of SIMS profiles showing a clear "plateau" effect[68] have given values of the same order as Eq. (B20) but a much more careful study of all evidence is needed.

---

*Permanent address: Department of Applied Physics, Stanford University, Stanford, CA 94305.

[1] C. Herring and N. M. Johnson, in *Hydrogen in Semiconductors*, edited by J. I. Pankove and N. M. Johnson, Vol. 34 of *Semiconductors and Semimetals*, Treatise Editors R. K. Willardson and A. C. Beer (Academic, Boston, 1991), Chap. 10.

[2] A. van Wieringen and N. Warmoltz, Physica (Amsterdam) **22**, 849 (1956).

[3] J. I. Pankove, D. E. Carlson, J. E. Berkeyheiser, and R. O. Wance, Phys. Rev. Lett. **51**, 2224 (1983); J. I. Pankove, R. O. Wance, and J. E. Berkeyheiser, Appl. Phys. Lett. **45**, 1100 (1984).

[4] N. M. Johnson, C. Herring, and D. J. Chadi, Phys. Rev. Lett. **56**, 769 (1986); *ibid.* **59**, 2116 (1987); N. M. Johnson and C. Herring, in Defects in Electronic Materials, edited by M. Stavola, S. J. Peartan, and G. Davis, Mater. Res. Soc. Symp. Proc. No. **104** (Materials Research Society, Pittsburgh, 1988), p. 277.

[5] Although theorists long ago speculated that two hydrogen atoms in silicon should be capable of combining into a stable H_2 complex similar to a free H_2 molecule, experimental evidence for such a complex consisted for many years solely in the fact that many workers were able to hydrogenate silicon so as to produce near-surface regions with hydrogen concentrations much larger than any possible contamination by other impurities, yet apparently uncharged, showing no spin resonance, and less strongly bound than expected for valence bonding with silicon. Only recently has an H_2 complex resembling a free molecule with slightly weaker binding been inferred from infrared and Raman evidence; see, e.g., B. Hourahine, R. Jones, S. Oberg, R. C. Newman, P. R. Briddon, and E. Roduner, Phys. Rev. B **57**, R12 666 (1998).

[6] C. H. Seager and R. A. Anderson, Appl. Phys. Lett. **53**, 1181 (1988); C. H. Seager, R. A. Anderson, and D. K. Brice, J. Appl. Phys. **68**, 3268 (1990).

[7] J. Zhu, N. M. Johnson, and C. Herring, Phys. Rev. B **41**, 12 354 (1990).

[8] N. M. Johnson and C. Herring, Phys. Rev. B **46**, 15 554 (1992).

[9] C. H. Seager, R. A. Anderson, and S. K. Estreicher, Phys. Rev. Lett. **74**, 4565 (1995).

[10] C. G. Van de Walle, P. J. H. Denteneer, Y. Bar-Yam, and S. T. Pantelides, Phys. Rev. B **39**, 10 791 (1989).

[11] C. G. Van de Walle, in *Hydrogen in Semiconductors*, edited by J. I. Pankove and N. M. Johnson, Vol. 34 of *Semiconductors and Semimetals*, Treatise Editors R. K. Willardson and A. C. Beer (Academic, Boston, 1991), p. 585.

[12] Yu. V. Gorelkinskii and N. N. Nevinnyi, Pis'ma Zh. Tekh. Fiz. **13**, 105 (1987) [Sov. Tech. Phys. Lett. **13**, 45 (1987)]; Physica B **170**, 155 (1991).

[13] R. F. Kiefl, M. Celio, T. L. Estle, S. R. Kreitzman, G. M. Luke, T. M. Riseman, and E. J. Ansaldo, Phys. Rev. Lett. **60**, 224 (1988).

[14] S. K. Estreicher, Mater. Sci. Eng., R. **14**, 319 (1995).

[15] P. J. H. Denteneer, C. G. Van de Walle, and S. T. Pantelides, Phys. Rev. B **41**, 3885 (1990).

[16] A. J. Tavendale, D. Alexiev, and A. A. Williams, Appl. Phys. Lett. **47**, 316 (1985); C. H. Seager and R. A. Anderson, in *Impurities, Defects, and Diffusion in Semiconductors: Bulk and Layered Structures*,'' edited by Donald J. Wolford, Jerzg Bernholc, and Eugene E. Haller, Mater. Res. Soc. Symp. Proc. No. **163** (Materials Research Society, Pittsburgh, PA, 1990), p. 431; T. Zundel, J. Weber, and L. Tilly, Physica B **170**, 361 (1991).

[17] N. M. Johnson and C. Herring, Phys. Rev. B **45**, 11 379 (1992).

[18] L. C. Kimerling, P. Blood, and W. M. Gibson, in Defects and radiation effects in semiconductors 1978, edited by J. H. Albany, IOP Conference Series No. **46** (Institute of Physics, London, 1979), p. 273.

[19] K. Irmscher, H. Klose, and K. Maass, J. Phys. C **17**, 6317 (1984).

[20] J. Frenkel, Phys. Rev. **54**, 647 (1938).

[21] B. Holm, K. Bonde Nielsen, and B. Bech Nielsen, Phys. Rev. Lett. **66**, 2360 (1991).

[22] Yu. V. Gorelkinskii and N. N. Nerinnyi, Physica B **170**, 155 (1991).

[23] B. Bech Nielsen, K. Bonde Nielsen, and J. R. Byberg, Mater. Sci. Forum **143–147**, 909 (1994).

[24] Yu V. Gorelkinskii and N. N. Nevinnyi, Mater. Sci. Eng., B **36**, 133 (1996).

[25] A. J Tavendale, S. J. Pearton, and A. A. Williams, Appl. Phys. Lett. **56**, 949 (1990).

[26] P. W. Anderson, Phys. Rev. Lett. **34**, 953 (1975).

[27] N. M. Johnson, C. Herring, and C. G. Van de Walle, Phys. Rev. Lett. **73**, 130 (1994); **74**, 1889(E) (1995).

[28] N. M. Johnson, in *Hydrogen in Semiconductors*, edited by J. I. Pankove and N. M. Johnson, Vol. 34 of *Semiconductors and Semimetals*, Treatise Editors R. K. Willardson and A. C. Beer (Academic, Boston, 1991), Chap. 7.

[29] D. V. Lang, J. Appl. Phys. **45**, 3014 (1974).

[30] W. K. Götz and N. M. Johnson, in *Characterization in Compound Semiconductor Processing*, edited by Y. Strausser and G. E. McGuire (Butterworth-Heinemann, Boston, 1995), Chap. 6.

[31] H. Lefevre and M. Schulz, Appl. Phys. **12**, 45 (1977).

[32] It should be noted that an alternative approach to the zero-field value of ε_D would be to devise an experimental determination of the mean energy $\langle \varepsilon \rangle$, which combined with ε_A would yield ε_D from $\langle \varepsilon \rangle \equiv (\varepsilon_D + \varepsilon_A)/2$.

[33] J. L. Hartke, J. Appl. Phys. **39**, 4871 (1968).

[34] The activation energies and prefactors are given to three significant figures in Eqs. (15) and (16) to ensure that these equations represent the data points in Fig. 11 to within the apparent accuracy of the latter. Because the probable errors in activation energies and prefactors are correlated, the error in either one by itself can be larger.

[35] P. Deák, L. C. Snyder, and J. W. Corbett, Phys. Rev. B **37**, 6887 (1988).

[36] Dj. M. Maric, S. Vogel, P. F. Meier, and S. K. Estreicher, Hyperfine Interact. **64**, 573 (1990).

[37] S. Estreicher, Phys. Rev. B **36**, 9122 (1987).

[38] In previous publications we have introduced the symbol H_2^* for the neutral, spinless form of hydrogen that is often found in *n*-type silicon hydrogenated below 300 °C and whose diffusion coefficient has been measured (Ref. 39). This is certainly the species relevant to our discussion in Secs. XIII and XIV of the present paper and probably in Sec. XII as well. As other recent literature uses the symbol H_2 uniformly for this species, we use H_2 also in this paper. Our previous use of two different symbols was an effort to distinguish this comparatively mobile species from a very stable and much less mobile hydrogen-containing complex generated during plasma hydrogenation of implanted *p-n* junctions. The nature of the latter complex has not yet been elucidated, but it now seems unlikely that it is the ground state for a pair of hydrogens in otherwise pure and perfect silicon. Also, our original meaning for the symbol H_2^* as the more mobile species has been confused by use of this same symbol for a hypothetical model complex consisting of two hydrogens at (roughly) bond-centered and antibonding positions [K. J. Chang and D. J. Chadi, Phys. Rev. B **40**, 11 644 (1989)]. While complexes of this type may under some conditions be formed and observed, we do not now believe that they play any role in the

experiments discussed in Secs. XII and XIV of the present paper.

[39] N. M. Johnson and C. Herring, Phys. Rev. B **43**, 14 297 (1991); C. Herring and N. M. Johnson, J. Appl. Phys. **87**, 4635 (2000).

[40] C. H. Seager, in *Hydrogen in Semiconductors*, edited by J. I. Pankove and N. M. Johnson, Vol. 34 of *Semiconductors and Semimetals*, Treatise Editors R. K. Willardson and A. C. Beer (Academic, Boston, 1991), Chap. 2.

[41] T. Zundel and J. Weber, Phys. Rev. B **39**, 13 549 (1989).

[42] N. M. Johnson, C. Herring, and C. G. Van de Walle, in *Proceedings of the 22th International Conference on the Physics of Semiconductors, Vancouver, 1994*, edited by D. J. Lockwood (World Scientific, Singapore), p. 2227.

[43] A. J. Tavendale, A. A. Williams, D. Alexiev, and S. J. Pearton, in Oxygen, Carbon, Hydrogen, and Nitrogen in Crystalline Silicon, edited by J. C. Mikkelsen, Jr., S. J. Pearton, J. W. Corbett and S. J. Pennycook, Mater. Res. Soc. Symp. Proc. No. 59 (Materials Research Society, Pittsburgh, PA, 1986), p. 469.

[44] C. H. Seager and R. A. Anderson, Appl. Phys. Lett. **59**, 585 (1991).

[45] T. Zundel and J. Weber, Phys. Rev. B **43**, 4361 (1991).

[46] K. Bonde Nielsen, B. Bech Nielsen, J. Hansen, E. Andersen, and J. U. Andersen, [Phys. Rev. B **60**, 1716 (1999)] have made the intriguing suggestion that at low temperature an H^0 can remain for some time metastable against transitions to its ground-state position at a bond center and during this time can diffuse very rapidly via transitions among other types of sites. Near room temperature, the region of interest to us, there is no metastability, so the bond-center site should be very predominantly occupied, though a diffusion constant thousands of times that of H^+ might be possible.

[47] C. Herring (unpublished).

[48] S. A. McQuaid, R. C. Newman, J. H. Tucker, E. C. Lightowlers, R. A. A. Kubiak, and M. Goulding, Appl. Phys. Lett. **58**, 2933 (1991).

[49] I. A. Veloarisoa, M. Stavola, D. M. Kozuch, R. E. Peale, and G. D. Watkins, Appl. Phys. Lett. **59**, 2121 (1991).

[50] S. A. McQuaid, M. J. Binns, R. C. Newman, E. C. Lightowlers, and J. B. Clegg, Appl. Phys. Lett. **62**, 1612 (1993).

[51] M. J. Binns, R. C. Newman, S. A. McQuaid, and E. C. Lightowlers, Mater. Sci. Forum **143–147**, 861 (1994).

[52] R. E. Pritchard, J. H. Tucker, R. C. Newman, and E. C. Lightowlers, Semicond. Sci. Technol. **14**, 77 (1999).

[53] A. W. R. Leitch, V. Alex, and J. Weber, Phys. Rev. Lett. **81**, 421 (1998).

[54] R. E. Pritchard, M. J. Ashwin, J. H. Tucker, and R. C. Newman, Phys. Rev. B **57**, R15 048 (1998).

[55] N. M. Johnson and C. Herring, Phys. Rev. B **43**, 14 297 (1991); V. P. Markevich and M. Suezawa, J. Appl. Phys. **83**, 2988 (1998); C. Herring and N. M. Johnson, *ibid.* **87**, 4635 (2000).

[56] G. G. DeLeo and W. B. Fowler, in *Hydrogen in Semiconductors*, edited by J. I. Pankove and N. M. Johnson, Vol. 34 of *Semiconductors and Semimetals*, Treatise Editors R. K. Willardson and A. C. Beer (Academic, Boston, 1991), Chap. 14; S. K. Estreicher, Mater. Sci. Eng., R. **14**, 319 (1995).

[57] Recent experiments indicate that H_2 prefers off-center positions in the region of low electron density surrounding the tetrahedral site, in which case the statistical factor $\nu_2 = 6$ in Table I should be replaced by a larger number; the effect on our numerical results in Secs. XII–XIV would be small. See J. A. Zhou and M. Stavola, [Phys. Rev. Lett. **83**, 1351 (1999)] and literature cited therein.

[58] N. M. Johnson, F. A. Ponce, R. A. Street, and R. J. Nemanich, Phys. Rev. B **35**, 4166 (1987).

[59] Chadi and Park [D. J. Chadi and C. H. Park, Phys. Rev. B **52**, 8877 (1995)] have pointed out that the Chang-Chadi complex (Ref. 38), being an electric dipole, might be expected to bind another H^+ or H^-, and have calculated a rather high binding energy for a linear $H_3{}^-$ complex. However, no experimental indication of such a species has been reported. In fact, the early finding that hydrogen could passivate donors (Ref. 4) was buttressed by the observation that hydrogenation increased the electron mobility by reducing the number of P^+ scattering centers, instead of decreasing the mobility by introducing negative ions. Thus, hydrogenation at 150 °C cannot have produced nearly as much $H_3{}^-$ as PH. So the binding energy calculated for $H_3{}^-$ by Chadi and Park must be much too high, and one can probably neglect this species in the present work.

[60] K. Bergman, M. Stavola, S. J. Pearton, and J. Lopata, Phys. Rev. B **37**, 2770 (1988).

[61] C. G. Van de Walle, Phys. Rev. B **49**, 4579 (1994); **58**, 1689(E) (1998).

[62] W. K. Leung, R. J. Needs, G. Rajagopal, S. Itoh, and S. Isahara, Phys. Rev. Lett. **83**, 2351 (1999).

[63] H. Reiss, C. S. Fuller, and F. J. Morin, Bell Syst. Tech. J. **35**, 535 (1956).

[64] C. Herring (unpublished).

[65] E. H. Rhoderick, *Metal-Semiconductor Contacts* (Oxford University Press, Oxford, 1978), Chap. 4.

[66] N. M. Johnson and C. Herring, Mater. Sci. Forum **143–147**, 867 (1994).

[67] C. Herring (unpublished).

[68] N. M. Johnson and C. Herring (unpublished).